Università degli Studi di Ferrara

Dipartimento di Ingegneria

Corso di Laurea Magistrale in Ingegneria Elettronica per l'ICT

Tecniche di decisione, stima e sensing distribuito.

Analysis of quantum illumination systems

Laureando
Federico Forzano

Relatore
Chiar.mo Prof. Andrea Conti

Correlatore
Dott. Ing. Andrea Giani

Anno Accademico 2022/2023

Sommario

Lo studio e la manipolazione delle proprietà quantistiche della radiazione elettromagnetica costituiscono elementi chiave per lo sviluppo di reti quantistiche per il sensing [1] e per le comunicazioni [2, 3, 4, 5, 6]. Tali reti sono composte da nodi in grado di acquisire informazioni riguardanti un sistema quantistico target e comunicare tra loro utilizzando stati quantistici associati alla radiazione elettromagnetica. Uno dei più promettenti protocolli di quantum sensing è la quantum illumination (QI) [7] che utilizza l'entanglement quantistico al fine di individuare la presenza di uno specifico target.

Un sistema di QI è tipicamente composto da tre elementi: trasmettitore, ricevitore e target. In particolare, il trasmettitore e il ricevitore fanno uso di due particelle completamente entangled (ad esempio fotoni), riferite abitualmente come particelle di segnale e ancilla, per effettuare il rilevamento. Nello specifico, il trasmettitore emette inizialmente la particella di segnale verso il target e contemporaneamente invia l'ancilla al ricevitore. Quest'ultimo, impiegando un'opportuna misurazione quantistica sul sistema composto dalle particelle di segnale e ancilla, è in grado di rilevare (se presente) il target. Il protocollo di QI è stato proposto e studiato utilizzando sia stati a singolo fotone [7, 8] che stati quantistici Gaussiani [9]. In entrambi i casi si è mostrato che è possibile ottenere performance significativamente migliori rispetto ai protocolli convenzionali descritti dall'elettrodinamica classica. Alcune applicazioni che possono trarre beneficio dall'utilizzo di sistemi di QI sono l'imaging in ambito biomedico, radar a bassa potenza, microscopia ottica a bassa potenza [10], ed il design di reti quantistiche.

Tuttavia, lo sviluppo di sistemi di QI è difficoltoso a causa di alcuni aspetti critici: (i) le tecnologie impiegate per la generazione degli stati entangled non sono ideali e pertanto non producono stati perfettamente entangled; (ii) l'entanglement è una proprietà estremamente sensibile agli effetti di decoerenza introdotti dalle non-idealità dei sistemi quantistici fisici reali; e (iii) la caratterizzazione matematica è ardua in quanto coinvolge espressioni che in generale non ammettono una soluzione in forma chiusa.

Gli obiettivi di questa tesi possono essere sintetizzati in: (i) studiare e analizzare la teoria della QI con stati quantistici a singolo fotone; (ii) estendere tale teoria al caso più generale in cui più di un fotone viene impiegato come ancilla; e (iii) individuare delle strategie di progetto per un sistema di QI con ancille multiple e compararne le performance con il sistema a singola ancilla. Lo studio condotto in questa tesi ha permesso di caratterizzare il compromesso tra il numero di fotoni di ancilla e il numero di shoots. Questo ha consentito l'individuazione della strategia ottima per il rilevamento di un target dato un budget energetico in termini di fotoni. In particolare, i risultati mostrano che il numero ottimale di fotoni ancilla è pari a uno anche in condizioni di livelli di rumore elevati.

Abstract

The exploitation of quantum mechanical properties of the electromagnetic radiation enables the next-generation quantum networks for sensing [1] and communications [2, 3, 4, 5, 6]. Such networks consist of distributed nodes that are capable of gathering informations about a target quantum system and communicate with each other by using quantum states. One of the most promising quantum sensing protocol is the quantum illumination (QI) [7], which exploits entanglement to detect the presence or the absence of a specific target.

A QI system is typically composed of three elements: transmitter, receiver and target. In particular, transmitter and receiver employ two fully entangled particles (e.g., photons), namely signal particle and ancilla particle, to perform target detection. Specifically, the transmitter initially shoots the target with the signal particle and then sends the ancilla one to the receiver. The latter, by performing a quantum measurement on the composite system of signal and ancilla, is able to detect (if present) the target. QI was investigated for single-photon states [7, 8] and Gaussian states [11]. In both cases, it can provide significant performance improvements with respect to conventional illumination (CI) protocols described by the classical electrodynamics. QI applications are envisioned to be employed in medical imaging, low-power short range radars, optical microscopy [10], and quantum networks.

However, characterizing QI protocols is challenging due to: (i) the employment of non-ideal technologies for generating and manipulating entangled quantum states that do not produce perfectly entangled states; (ii) entanglement degradation caused by decoherence effects introduced by non-ideal quantum systems; and (iii) difficult mathematical characterization involving cumbersome expressions that, in general, do not admit closed-forms.

The goals of this thesis are: (i) study of the theory of QI with single-photon states; (ii) extend single-photon QI to the case with multiple ancilla photons; and (iii) establish design strategies for QI with multiple ancillas and compare their performance with that provided by QI with a single ancilla. This work allows to characterize the tradeoff between the number of shoots and the number of ancilla photons. Results show that for a given budget of photons, the optimal strategy for QI is that one with single ancilla photon, even in the presence of noise.

Contents

Acronyms

CI conventional illumination

MSE mean square error

OOK on-off keying

PDF probability density function

POVM positive operator valued measure

QCB quantum Chernoff bound

QCRB quantum Cramèr-Rao bound

QI quantum illumination

QM quantum mechanics

QSD quantum state discrimination

RV random variable

SHO simple harmonic oscillator

SLD symmetrized logarithmic derivative

SPDC spontaneous parametric down-conversion

Chapter 1

Introduction

In a world where information is becoming increasingly ubiquitous and play a central role in our lives, the capabilities of sensing the environment and inferring physical quantities are fundamental tasks to design high-performance systems. Conventional sensing systems rely on a classical electrodinamical description of both the electromagnetic field and its interaction with matter. However, such description exhibits limitations due to the unmodeled aspects of the microscopical physical world. In this context, quantum information science aims to overcome these limitations by harnessing the quantum mechanical properties of the radiation to design technologies, algorithms, and protocols with better performance and unique features.

In particular, quantum sensing is a promising field of quantum information science that leverages quantum mechanical properties, such as superposition and entanglement, to infer physical quantities associated to a target system. Quantum sensing has found applications in various domains, including quantum illumination [7], quantum ranging [12], quantum metrology [13], and quantum tomography [14]. Potential applications of quantum sensing are extensive and span multiple fields, including quantum networks. For instance, in [15], it is demonstrated that quantum sensing can enhance measurement accuracy in quantum key distribution, thus improving communication security. In [16, 17], quantum sensing is employed to estimate decoherence effects observed in non-ideal quantum channels. Moreover, in [18], quantum metrology is shown to be fundamental to synchronize the cooperation of nodes in quantum sensing and communication networks. Quantum sensing also enables enhanced positioning systems [19, 20], including quantum ranging and quantum target detection. In particular, in [7], the QI protocol is proposed to perform target detection, i.e., the process of detecting the presence or the absence of a target.

QI has garnered significant interest since it overcomes limitations of CI methods and allows to design systems capables of detecting targets with low-power signals even in the presence of high levels of noise. The central idea is to employ an ancillary electromagnetic radiation to enhance the detection performance. It has been demonstrated that if such ancilla is entangled with the signal radiation, the detection error probability can be reduced.

This thesis explores QI and some relevant variants. In particular, after providing some preliminaries on the quantization of the electromagnetic field and quantum decision theory, common QI techniques with single-photon states and their variants are investigated. Then, QI with single-photon states is extended to the case of multiple ancilla photons. In particular, design strategies for QI systems with multiple ancilla photons and a given power budget (in terms of number of photons) are presented. Finally, the performance of QI with multiple ancillas are compared with that of QI with single ancilla. Numerical results show that the optimal detection strategy is achieved when employing only one ancilla photon, even in the

presence of high noise intensity. Moreover, it is shown that when performing QI with a given budget of photons, there exists a tradeoff between the number of ancillas per shots and the number of shots.

This thesis is organized as follows:

Chapter 2 provides some preliminaries on quantum mechanics (QM) with particular attention to the Dirac-Von Neumann postulates and the quantum description of the electromagnetic field.

Chapter 3 discusses quantum decision and estimation theory and presents important results, including the Helstrom bound, quantum Chernoff bound (QCB), and quantum Cramèr-Rao bound (QCRB).

Chapter 4 firstly presents QI with single-photon states and generalizes it to the case with multiple ancilla photons. Then, it evaluates and compares the performance of such protocols, even accounting for a budget of photons. Finally, it discusses the optimal tradeoff between number of ancilla photons per shoot and number of shoots.

Chapter 5 provides the conclusions.

Notation

Operators are denoted by bold uppercase letters. Vectors are denoted by bold lowercase letters. The sets of complex and real numbers are denoted by $\mathbb{C}$ and $\mathbb{R}$, respectively. For $z \in \mathbb{C}$: $|z|$ and $\arg(z)$ dentote the absolute value and the argument; z^* is the complex conjugate. The trace and the adjoint of an operator are denoted by $\mathrm{tr}\{\cdot\}$ and $(\cdot)^\dagger$, respectively. Random variables are displayed in sans serif, upright fonts; their realizations in serif, italic fonts. For example, a random variable and its realization are denoted by x and x; a random operator and its realization are denoted by $\mathbf{X}$ and $\boldsymbol{X}$, respectively. The Kronecker delta function, the discrete delta function, and the generalized delta function are denoted by $\delta_{n,m}$, δ_n, and $\delta(\cdot)$, respectively.

Chapter 2

Fundamentals of quantum mechanics

To understand the important innovations that will be described in this thesis, it is essential to be familiar with the key aspects of QM and with its mathematical framework. In contrast to the rigor of mathematical formulations, the physical implications of this theory are hard to imagine and depart from daily perception. In this thesis, some important results will firstly be presented mathematically and then their physical implications are discussed.

2.1 Postulates

The origin of QM lies in experimental observations such as the black-body radiation [21], the photoelectric effect [22], the diffration experiment [23], and the Brownian motion [24]. Contrary to the difficulty of explaining such phenomena, QM can be formulated with few elementary postulates. Nevertheless, the mathematical formulation of the theory is not unique and in this thesis are described the Dirac-Von Neumann postulates [25, 26] in the Schrödinger's picture. The postulates completely characterize the QM theory in four key concept: the system state, the evolution of the state, the quantum measurements, and the composition of two or more systems. With Schrödinger's picture is refered the description of quantum systems with time-dependent states and time-indipendent measurement operators.

2.1.1 First postulate: system state

> *The state of an isolated quantum system is represented by a complex unitary vector $|\psi\rangle \in \mathcal{H}$. The space of possible states of the system $\mathcal{H}$ is called state space and it is a separable complex Hilbert space.*

From the perspective of QM, a mechanical system is completely described by a state. The state is a complex vector (in general time-dependent) and it is not an observable property like speed, position or any other conventional physical quantity. The reasons for introducing a state vector will be better complemented by the presentation of the first three postulates.

The notation used before is called Dirac's notation: a state vector is indicated by the ket notation $|\cdot\rangle$; its dual vector is called bra-vector and is indicated by $\langle\cdot|$ (if the $|\psi\rangle$ is finite-dimensional, the dual vector $\langle\psi|$ is simply its transposed conjugate). The inner product between two vectors $|\alpha\rangle$ and $|\beta\rangle$ is written as $\langle\alpha|\beta\rangle$.

If the state of the system is not completely known and there is an ensemble of possible states

with the associated probabilities:

$$\{(|\psi_1\rangle, p_1), (|\psi_2\rangle, p_2), \ldots, (|\psi_n\rangle, p_n)\}$$

it is possible to define a **density operator** $\boldsymbol{\Xi} \in \mathcal{L}(\mathcal{H})$ (acting on the space $\mathcal{H}$, i.e. $\boldsymbol{\Xi} = \mathcal{H} \to \mathcal{H}$) as it follows:

$$\boldsymbol{\Xi} \coloneqq \sum_{i=1}^{n} p_i \, |\psi_i\rangle\langle\psi_i| \, . \tag{2.1}$$

A quantum state that is not perfectly known (as before) is called **mixed state** in opposition of the exactly known quantum state that is called **pure state**. It is also possible to define a density operator for a pure state $|\psi\rangle$ as $\boldsymbol{\Xi} = |\psi\rangle\langle\psi|$ and it is possible to check if a state is pure from its density operator: a pure state's density operators satisfy $\mathrm{tr}\{\boldsymbol{\Xi}^2\} = 1$, while mixed state's density operators has $\mathrm{tr}\{\boldsymbol{\Xi}^2\} < 1$.

The density operator $\boldsymbol{\Xi}$ provides a complete statistical description of a quantum mechanical system and has the following properties: $\boldsymbol{\Xi}$ is Hermitian, i.e., $\boldsymbol{\Xi} = \boldsymbol{\Xi}^\dagger$, and it has unitary trace, i.e., $\mathrm{tr}\{\boldsymbol{\Xi}\} = 1$. It is easy to show that if a quantum system can be in states $\{\boldsymbol{\Xi}_i\}_i$ with probabilities $\{p_i\}_i$, the density operator associated to it is given by:

$$\boldsymbol{\Xi} = \sum_i p_i \, \boldsymbol{\Xi}_i \, . \tag{2.2}$$

2.1.2 Second postulate: time evolution

The evolution of an isolated quantum system from time t_0 to t_1 is described by an unitary operator $\boldsymbol{U} \in \mathcal{L}(\mathcal{H})$ that depends only from the system at times t_0 and t_1:

$$|\psi(t_1)\rangle = \boldsymbol{U}(t_0, t_1) \, |\psi(t_0)\rangle \, .$$

Since the state of the system is not an observable property, its time-evolution cannot be easily imagined as the unitary operator $\boldsymbol{U}$ has not a easy interpretation. The time-evolution of quantum states can be rewritten in the formalism of the partial-derivative equations for a continuous-time evolution. The equation that will be described in the following lines is called **Schrödinger equation** and is one of the most important equations of the QM:

$$\imath\hbar \frac{\partial |\psi\rangle}{\partial t} = \boldsymbol{H} \, |\psi\rangle \, . \tag{2.3}$$

The Schrödinger equation 2.3 describes the continuous-time evolution of the state vector $|\psi\rangle$. The constant $\hbar$ is called reduced Planck's constant, $\imath$ is the immaginary unit ($\imath^2 = -1$), and $\boldsymbol{H}$ is the Hamiltonian operator of the quantum mechanical system. The Hamiltonian is an Hermitian operator and its eigenvalues are the admitted energy levels of the system:

$$\boldsymbol{H} \, |E\rangle = E \, |E\rangle \, . \tag{2.4}$$

The relation between discrete and continuous equations of the state time-evolution are given by the solution of the Schrödinger's equation:

$$|\psi(t_1)\rangle = \exp\left\{ \frac{-\imath \, \boldsymbol{H}(t_1 - t_0)}{\hbar} \right\} |\psi(t_0)\rangle = \boldsymbol{U}(t_0, t_1) \, |\psi(t_0)\rangle \, . \tag{2.5}$$

It can be proven that the evolution for a system described by the density operator $\boldsymbol{\Xi}$ under the effect of the unitary operator $\boldsymbol{U}$ is given by:

$$\boldsymbol{\Xi}(t_1) = \boldsymbol{U}(t_0, t_1) \, \boldsymbol{\Xi}(t_0) \, \boldsymbol{U}^\dagger(t_0, t_1) \, . \tag{2.6}$$

2.1.3 Third postulate: quantum measurements

A quantum measurement is described by a set of measurement operators $\{\boldsymbol{M}_m\}$ acting on the state space $\mathcal{H}$, where m are the possible outocomes of the measurement. The probability that result m occurs is:

$$\mathbb{P}\{m\} = \langle\psi|\ \boldsymbol{M}_m^\dagger\, \boldsymbol{M}_m\ |\psi\rangle \tag{2.7}$$

and the state of the system after the measurement with outcome m is

$$|\psi'\rangle = \frac{\boldsymbol{M}_m\ |\psi\rangle}{\sqrt{\langle\psi|\ \boldsymbol{M}_m^\dagger\, \boldsymbol{M}_m\ |\psi\rangle}}\,. \tag{2.8}$$

Since the probabilities have to sum to one, the measurement operators have to satisfy the completeness equation:

$$\sum_m \boldsymbol{M}_m^\dagger\, \boldsymbol{M}_m = \boldsymbol{I}\,, \tag{2.9}$$

where $\boldsymbol{I}$ is the identity operator.

It is now possible to highlight one crucial aspect of the quantum mechanical theory: *QM is not a deterministic theory.* A quantum mechanical system is something that we cannot describe as a common-experience system; we can measure only some observables of the system and outcomes of the measurements are not deterministic. Moreover, the measurement's result not only depends on the system state but also on the measuring system (that determines the measurement operators) and it is not possible to interact with a quantum system without disturbing it.

However, it is possible to note that the measurement operators $\boldsymbol{M}_m$ are useful only to determine the state after the relative measurements. For some applications, the post-measurement state of the system is of little interest and the main focus of concern are the probabilities of the respective measurement outcomes. In such instances it is useful to introduce a mathematical tool known as **positive operator valued measure (POVM) formalism**. Let's suppose that a measurement performed on a quantum system in the state $|\psi\rangle$ is described by the measurement operators $\{\boldsymbol{M}_m\}$. Then, the probability that outcome m occurs is given by the equation 2.7. Defining an operator

$$\boldsymbol{\Pi}_m \coloneqq \boldsymbol{M}_m^\dagger\, \boldsymbol{M}_m \tag{2.10}$$

we have that $\boldsymbol{\Pi}_m$ is a positive operator, $\mathbb{P}\{m\} = \langle\psi|\, \boldsymbol{\Pi}_m\, |\psi\rangle$, and $\sum_m \boldsymbol{\Pi}_m = \boldsymbol{I}$. The set $\{\boldsymbol{\Pi}_m\}$ is sufficient to determine the outcome probabilities and it is known as POVM.

Projective measurements

A projective measurement on the system in the state $|\psi\rangle \in \mathcal{H}$ is a quantum measurement that can be described by an observable operator $\boldsymbol{M} \in \mathcal{L}(\mathcal{H})$. The observable operator is Hermitian and has spectral decomposition

$$\boldsymbol{M} = \sum_m m\, \boldsymbol{P}_m \tag{2.11}$$

where $\boldsymbol{P}_m$ are the projectors onto the eigenspace of $\boldsymbol{M}$ with eigenvalues m. Possible outcomes of the measurement are the eigenvalues m and the outcome probabilities are given by

$$\mathbb{P}\{m\} = \langle\psi|\boldsymbol{P}_m|\psi\rangle\ . \tag{2.12}$$

The state of the system after the measurement is

$$|\psi'\rangle = \frac{\boldsymbol{P}_m\, |\psi\rangle}{\sqrt{\langle\psi|\boldsymbol{P}_m|\psi\rangle}}\,, \tag{2.13}$$

which means that the system state collapses to the eigenstate associated to the measured eigenvalue. The main advantage of a projective measurement is that it is easy to calculate its expected value that is denote as $\langle \boldsymbol{M} \rangle$ and can be obtained as:

$$\langle \boldsymbol{M} \rangle = \sum_m m \, \mathbb{P}\{m\} \tag{2.14a}$$

$$= \langle \psi | \boldsymbol{M} | \psi \rangle \ . \tag{2.14b}$$

Heisenberg uncertainty principle

The uncertainty principle is anotherone important result of QM since it defines the ultimate boundary of precision for the measurement of two observables of the same system. In this thesis is briefly described the statement of this principle, a proof in the same formalism of this work can be found in [27].

Let's suppose that $\boldsymbol{A}$ and $\boldsymbol{B}$ are two observables of a quantum system in the state $|\psi\rangle$ and denote as $(\Delta \boldsymbol{A})^2 = \langle (\boldsymbol{A} - \langle \boldsymbol{A} \rangle)^2 \rangle$ the variance of the measurement outcome of the observable $\boldsymbol{A}$ (in the same way is defined the variance of $\boldsymbol{B}$). The Heisenberg principle can be formulated as it follows:

$$\Delta \boldsymbol{A} \, \Delta \boldsymbol{B} \geq \frac{1}{2} \langle [\boldsymbol{A}, \boldsymbol{B}] \rangle \, , \tag{2.15}$$

where $[\boldsymbol{A}, \boldsymbol{B}] \coloneqq \boldsymbol{A}\,\boldsymbol{B} - \boldsymbol{B}\,\boldsymbol{A}$ is called commutator of $\boldsymbol{A}$ and $\boldsymbol{B}$. The interpretation of the previous result can be given as it follows: the precision, measuring two observables of the same system, is always lower-bounded and the bound depends on the nature of the observables. A deep knowledge of one of the two observables involves a poor knowledge of the other one.

Note also that the uncertainty must not be attributed to the measurement process, i.e., to the perturbation of the system due to the measurement. It should rather be interpreted as it follows: given a set of quantum systems in identical states and performing a measurement of $\boldsymbol{A}$ in half systems and $\boldsymbol{B}$ in the others, the uncertainty of the two measurements have to satisfy the inequation 2.15. The measurement uncertainty is then a property of the microscopic world and it does not depend on human limitations or on nonideal experimental setups.

Measurements on mixed states

The measurement's postulate can be revised in terms of density operators using the total probability law as it follows:

$$\mathbb{P}\{m\} = \sum_i p_i \, \mathbb{P}\{m|i\} \tag{2.16a}$$

$$= \sum_i p_i \ \mathrm{tr}\big\{ \boldsymbol{M}_m^\dagger \, \boldsymbol{M}_m \ |\psi_i\rangle\langle\psi_i| \big\} \tag{2.16b}$$

$$= \mathrm{tr}\big\{ \boldsymbol{M}_m^\dagger \, \boldsymbol{M}_m \, \boldsymbol{\Xi} \big\} \tag{2.16c}$$

where the expression two is obtained considering that $\langle \psi | \boldsymbol{A} | \psi \rangle = \mathrm{tr}\{ \boldsymbol{A} \ |\psi\rangle\langle\psi| \}$ for every operator $\boldsymbol{A}$. In a similar way, using the conditional probability Bayes rule, it is possible to show that the state after measuring the outcome m results

$$\boldsymbol{\Xi}' = \frac{\boldsymbol{M}_m \, \boldsymbol{\Xi} \, \boldsymbol{M}_m^\dagger}{\mathrm{tr}\Big\{ \boldsymbol{M}_m^\dagger \, \boldsymbol{M}_m \, \boldsymbol{\Xi} \Big\}} \, . \tag{2.17}$$

2.1.4 Fourth postulate: composite systems

The state space of a composite quantum system is given by the tensor product of the state spaces of the component physical systems, i.e., if the component systems has state spaces $\mathcal{H}_1$, $\mathcal{H}_2$, ..., $\mathcal{H}_n$, the composite system has state space

$$\mathcal{H} = \mathcal{H}_1 \otimes \mathcal{H}_2 \otimes \cdots \otimes \mathcal{H}_n \,.$$

The last postulate leads to one of the most intriguing and controversial aspects of QM: the **quantum entanglement**. Let's introduce this counter-intuitive concept with an example. Consider two qubit systems: system A with state space $\mathcal{H}_\mathrm{A}$ and system B with state space $\mathcal{H}_\mathrm{B}$ (a qubit is the easiest quantum system with a two-dimensional state space). Denote as $\{\,|0_\mathrm{A}\rangle\,,\ |1_\mathrm{A}\rangle\}$ and $\{\,|0_\mathrm{B}\rangle\,,\ |1_\mathrm{B}\rangle\}$ respectively a basis of system A and system B. Let's suppose that the systems are in the states

$$|\psi_\mathrm{A}\rangle = \frac{1}{\sqrt{2}}\,(\,|0_\mathrm{A}\rangle + |1_\mathrm{A}\rangle) \tag{2.18a}$$

$$|\psi_\mathrm{B}\rangle = \frac{1}{\sqrt{2}}\,(\,|0_\mathrm{B}\rangle + |1_\mathrm{B}\rangle) \tag{2.18b}$$

and consider the composite system with state

$$|\psi_1\rangle = |\psi_\mathrm{A}\rangle \otimes |\psi_\mathrm{B}\rangle = \frac{1}{2}\,(\,|0_\mathrm{A}, 0_\mathrm{B}\rangle + |0_\mathrm{A}, 1_\mathrm{B}\rangle + |1_\mathrm{A}, 0_\mathrm{B}\rangle + |1_\mathrm{A}, 1_\mathrm{B}\rangle)\,. \tag{2.19}$$

A state that can be obtained as a tensor product of two state is called **product state**. Performing a measurement on the system B we can expect that the system A will be unaffected. This is perfectly justified by the fact that the two qubits could be in a different place and they cannot necessarily comunicate with eachother. Suppose that a measure on A results 0, the systems collapse (for the third postulate 2.13) in the state $|\psi_1'\rangle = \frac{1}{\sqrt{2}}\,(\,|0_\mathrm{A}, 0_\mathrm{B}\rangle + |0_\mathrm{A}, 1_\mathrm{B}\rangle) = |0_\mathrm{A}\rangle \otimes |\psi_\mathrm{B}\rangle$ and then the state B is unaffected.

Consider now a second composite system and suppose that it is in the state

$$|\psi_2\rangle = \frac{1}{\sqrt{2}}\,(\,|0_\mathrm{A}, 1_\mathrm{B}\rangle - |1_\mathrm{A}, 0_\mathrm{B}\rangle)\,. \tag{2.20}$$

The first observation is that the state cannot be written as a tensor product of two states; such states are called **entangled states**. If a measurement on the system A results 0, the system collapses in $|\psi_2'\rangle = |0_\mathrm{A}, 1_\mathrm{B}\rangle$ which means that the system B is affected by the measurement on A.

This property of quantum systems was central in the scientific debate in the early 1900s and Einstein was the most well-known person to be involved in it. He, together with Podolsky and Rosen in 1935 [28], claims that the theory cannot be complete because it does not satisfy two requirements: (i) the properties of a physical system are inherent in the system itself, and should thus exist before any measurement is made (*realism*), and (ii) that no signal can travel faster than light (*locality*). Their conclusion is that there must exist some hidden variables not considered by QM and then it must be incomplete (LHV theory). The LHV theory was refuted thanks to the experiment proposed by Bell in 1964 [29] and Clauser, Horne, Shimony, and Holt (CHSH) in 1969 [30] and implemented by Aspect in 1982 [31]. Quantum mechanics is a complete theory and the microscopic world has not the properties of locality and reality. Therefore, no LHV theory can obtain all the QM results.

2.2 The quantum theory of light

The study of light's microscopic nature was one of the first topic that led to the formulation of quantum theory. The publication of Einstein's paper on photoelectric effect [22] made it

clear that the electromagnetic radiation must have a corpuscular nature, nevertheless provide a rigorous description of that in terms of QM laws required several years.

QM theory assumes that electromagnetic radiation consists of quantum particles called *photons*. Like every quantum particle, a photon can be completely described by it state vector (or by a wavefunction $\psi(\boldsymbol{r}, t) = \boldsymbol{Q}\,|\psi(t)\rangle$, where $\boldsymbol{Q}$ is the position operator) but is outside the scope of this thesis to find that [32]. This section aims to provide a description of the electromagnetic radiation in terms of photons and highlights the main analogies and differences with the classical view.

2.2.1 Classical description of the electromagnetic radiation

In the quantum vision, the electric and magnetic fields are considered observables of a quantum system and they are thus described with operators. In order to define such operators we firstly revise the classical description of the electromagnetic radiation and then we briefly show how it can be derived the Hamiltonian of the field. Quantum operators corresponding to the fields can be found with the canonical quantization procedure that will be described in the following section.

Firstly, let's proceed from the time-dependent Maxwell equations to find a quantum description of the EM radiation.

$$\nabla \times \boldsymbol{\mathcal{E}} = -\frac{\partial \boldsymbol{\mathcal{B}}}{\partial t} \tag{2.21a}$$

$$\nabla \times \boldsymbol{\mathcal{E}} = \mu_0 \boldsymbol{J} + \frac{1}{c^2}\frac{\partial \boldsymbol{\mathcal{E}}}{\partial t} \tag{2.21b}$$

$$\nabla \cdot \boldsymbol{\mathcal{E}} = \frac{\rho}{\epsilon_0} \tag{2.21c}$$

$$\nabla \cdot \boldsymbol{\mathcal{B}} = 0 \tag{2.21d}$$

The well known Maxwell equations 2.21 describe the electromagnetic radiation as vectorial fields $\boldsymbol{\mathcal{E}}(\boldsymbol{r}, t)$ and $\boldsymbol{\mathcal{B}}(\boldsymbol{r}, t)$ (the position $\boldsymbol{r}$ and time t dependence are omitted in the equations 2.21 only for simplicity). The current density vector $\boldsymbol{J}$ and the volumetric charge density ρ are the sources of the field.

In order to simplify the calculation, let study the field without sources ($\boldsymbol{J} = 0$ and $\rho = 0$). The divergency equation become

$$\nabla \cdot \boldsymbol{\mathcal{E}} = 0 \tag{2.22a}$$

$$\nabla \cdot \boldsymbol{\mathcal{B}} = 0\,. \tag{2.22b}$$

Define a couple of a vector and scalar potentials ($\boldsymbol{\mathcal{A}}$, Φ) such that the fields are given by:

$$\boldsymbol{\mathcal{E}} = -\nabla\Phi - \frac{\partial \boldsymbol{\mathcal{A}}}{\partial t} \tag{2.23a}$$

$$\boldsymbol{\mathcal{B}} = \nabla \times \boldsymbol{\mathcal{A}}\,, \tag{2.23b}$$

with $\boldsymbol{\mathcal{A}}$ and Φ that depends on the time t and the position $\boldsymbol{r}$. The possible choices for $(\boldsymbol{\mathcal{A}}, \Phi)$ are infinite and we set without loss of generality

$$\nabla \cdot \boldsymbol{\mathcal{A}} = 0 \tag{2.24a}$$

$$\Phi = 0\,. \tag{2.24b}$$

The potentials that satisfy this conditions are called *Coulomb gauge*. The fields are then given by:

$$\boldsymbol{\mathcal{E}} = -\frac{\partial \boldsymbol{\mathcal{A}}}{\partial t} \tag{2.25a}$$

$$\boldsymbol{\mathcal{B}} = \nabla \times \boldsymbol{\mathcal{A}}\,. \tag{2.25b}$$

In order to solve the curl equations we need to specify the boundary conditions of the problem. If we study the EM radiation inside a cubic PEC cavity with L-side, we have a numerable infinity of solution that can be expressed in the following form:

$$\boldsymbol{\mathcal{A}}_{\boldsymbol{k}}(\boldsymbol{r},\, t) = A_{\boldsymbol{k}}\, \hat{\boldsymbol{e}}_{\boldsymbol{k}}\, e^{\imath(\boldsymbol{k}\cdot\boldsymbol{r}-\omega\, t)} + A_{\boldsymbol{k}}\, \hat{\boldsymbol{e}}^{*}_{\boldsymbol{k}}\, e^{-\imath(\boldsymbol{k}\cdot\boldsymbol{r}-\omega\, t)} \tag{2.26}$$

where $\boldsymbol{k} = k_x\, \hat{\boldsymbol{x}} + k_y\, \hat{\boldsymbol{y}} + k_z\, \hat{\boldsymbol{z}}$ is the propagation vector that satisfy $k^2 = \|\boldsymbol{k}\|^2 = \frac{\omega^2}{c^2}$ and $\boldsymbol{r} = x\, \hat{\boldsymbol{x}} + y\, \hat{\boldsymbol{y}} + z\, \hat{\boldsymbol{z}}$. From the boundary contitions we obtain $k_x = \frac{2\,\pi}{L}\, n_1$, $k_y = \frac{2\,\pi}{L}\, n_2$ and $k_z = \frac{2\,\pi}{L}\, n_3$ where $n_1, n_2, n_3 \in \mathbb{Z}$. From $\nabla \cdot \boldsymbol{\mathcal{A}}_{\boldsymbol{k}} = 0$ we obtain that $\nabla \cdot \hat{\boldsymbol{e}}_{\boldsymbol{k}} = 0$. The vector $\hat{\boldsymbol{e}}_{\boldsymbol{k}}$ represent the polarization vector, it has unitary norm and it is always orthogonal to the propagation vector $\boldsymbol{k}$. Defining an orthonormal bases of the polarization plane $\{\hat{\boldsymbol{e}}_{\boldsymbol{k},\,1}, \hat{\boldsymbol{e}}_{\boldsymbol{k},\,2}\}$. The vectors $\hat{\boldsymbol{e}}_{\boldsymbol{k},\,\sigma}$ satisfy

$$\hat{\boldsymbol{e}}_{\boldsymbol{k},\,\sigma} \cdot \hat{\boldsymbol{e}}_{\boldsymbol{k}',\,\sigma'} = \delta_{\boldsymbol{k},\,\boldsymbol{k}'}\, \delta_{\sigma,\,\sigma'} \tag{2.27}$$

The potential vector $\boldsymbol{\mathcal{A}}(\boldsymbol{r},\, t)$ can be written as:

$$\boldsymbol{\mathcal{A}}(\boldsymbol{r},\, t) = \sum_{\substack{\boldsymbol{k} \\ \sigma\in\{1,\,2\}}} A_{\boldsymbol{k}}\, a_{\boldsymbol{k},\,\sigma}\, \hat{\boldsymbol{e}}_{\boldsymbol{k},\,\sigma}\, e^{\imath(\boldsymbol{k}\cdot\boldsymbol{r}-\omega\, t)} + A_{\boldsymbol{k}}\, a^{*}_{\boldsymbol{k},\,\sigma}\, \hat{\boldsymbol{e}}_{\boldsymbol{k},\,\sigma}\, e^{-\imath(\boldsymbol{k}\cdot\boldsymbol{r}-\omega\, t)}\,. \tag{2.28}$$

The electric and magnetic fields can be calculated from the equations 2.25 replacing the vector $\boldsymbol{\mathcal{A}}(\boldsymbol{r},\, t)$ with the expression 2.28. It results:

$$\boldsymbol{\mathcal{E}}(\boldsymbol{r},\, t) = \frac{\partial \boldsymbol{\mathcal{A}}(\boldsymbol{r},\, t)}{\partial t} \tag{2.29a}$$

$$= \sum_{\boldsymbol{k}} \sum_{\sigma} \imath\, A_{\boldsymbol{k}}\, \omega_{\boldsymbol{k}} \left[a_{\boldsymbol{k},\,\sigma}\, \hat{\boldsymbol{e}}_{\boldsymbol{k},\,\sigma}\, e^{\imath\,(\boldsymbol{k}\cdot\boldsymbol{r}-\omega_{\boldsymbol{k}}\, t)} - a^{*}_{\boldsymbol{k},\,\sigma}\, \hat{\boldsymbol{e}}_{\boldsymbol{k},\,\sigma}\, e^{-\imath\,(\boldsymbol{k}\cdot\boldsymbol{r}-\omega_{\boldsymbol{k}}\, t)}\right] \tag{2.29b}$$

$$\boldsymbol{\mathcal{B}}(\boldsymbol{r},\, t) = \nabla \times \boldsymbol{\mathcal{A}}(\boldsymbol{r},\, t) \tag{2.29c}$$

$$= \sum_{\boldsymbol{k}} \sum_{\sigma} \imath\, A_{\boldsymbol{k}}\, k \left[\hat{\boldsymbol{k}} \times \hat{\boldsymbol{e}}_{\boldsymbol{k},\,\sigma}\, a_{\boldsymbol{k},\,\sigma}\, e^{\imath\,(\boldsymbol{k}\cdot\boldsymbol{r}-\omega_{\boldsymbol{k}}\, t)} - \hat{\boldsymbol{k}} \times \hat{\boldsymbol{e}}_{\boldsymbol{k},\,\sigma}\, a^{*}_{\boldsymbol{k},\,\sigma}\, e^{-\imath\,(\boldsymbol{k}\cdot\boldsymbol{r}-\omega_{\boldsymbol{k}}\, t)}\right]. \tag{2.29d}$$

The Hamiltonian of the electromagnetic field inside the cavity can be calculated as its the total energy, i.e., as the integral of the Poynting vector over all the volume of the cavity:

$$H = \iiint_{[0,\,L]^3} \frac{1}{2}\, \epsilon_0\, \boldsymbol{\mathcal{E}} \cdot \boldsymbol{\mathcal{E}} + \frac{1}{2\,\mu_0}\, \boldsymbol{\mathcal{B}} \cdot \boldsymbol{\mathcal{B}}\, dV \tag{2.30a}$$

$$= \sum_{\boldsymbol{k},\,\sigma} \epsilon_0\, A^2_{\boldsymbol{k}}\, \omega^2_{\boldsymbol{k}}\, V \left[a_{\boldsymbol{k},\,\sigma}\, a^{*}_{\boldsymbol{k},\,\sigma} + a^{*}_{\boldsymbol{k},\,\sigma}\, a_{\boldsymbol{k},\,\sigma}\right], \tag{2.30b}$$

where $V = L^3$ is the volume of the cavity.

2.2.2 Quantization of the simple harmonic oscillator

The mono-dimensional simple harmonic oscillator (SHO) quantization is one of the standard problems of quantum physics. In this thesis is briefly described the quantization procedure of this type of system and are highlighted some affinities with the electromagnetic radiation quantization problem.

The starting point to provide a quantum description of a system is to define its Hamiltonian. A SHO is a physical system governed by the equation

$$\ddot{q} + \omega^2\, q = 0\,, \tag{2.31}$$

where q is the position and the notation $\ddot{q}$ denote the second order time derivative of the position. The potential energy of a SHO is given by the expression

$$U = \frac{1}{2}\, k\, q^2\,, \tag{2.32}$$

where $k = \omega^2 m$ and m is the mass of the object. The classical Hamiltonian of the system can be calculated as the sum of kinetic and potential energies and results

$$H = \frac{p^2}{2m} + \frac{1}{2} k q^2 , \tag{2.33}$$

where p is the momentum.

The canonical quantization of the system is obtained by replacing momentum and position observables with the two correspondent quantum operators

$$q \to \boldsymbol{Q} \tag{2.34a}$$

$$p \to \boldsymbol{P} \tag{2.34b}$$

acting on the state space $\mathcal{H}$ of the system. The operators $\boldsymbol{Q}$ and $\boldsymbol{P}$ satisfy the canonical commutation relation

$$[\boldsymbol{P}, \boldsymbol{Q}] = \boldsymbol{P}\boldsymbol{Q} - \boldsymbol{Q}\boldsymbol{P} = -i\hbar . \tag{2.35}$$

The quantum Hamiltonian operator results

$$\boldsymbol{H} = \frac{\boldsymbol{P}^2}{2m} + \frac{1}{2} k \boldsymbol{Q}^2 \tag{2.36a}$$

$$= \frac{\boldsymbol{P}^2}{2m} + \frac{1}{2} m\omega^2 \boldsymbol{Q}^2 . \tag{2.36b}$$

It is then useful to define two new operators called **annihilation operator** ($\boldsymbol{A}$) and **creation operator** ($\boldsymbol{A}^\dagger$) defined as

$$\boldsymbol{A} \coloneqq \frac{1}{\sqrt{2m\omega\hbar}} (m\omega \boldsymbol{Q} + \imath \boldsymbol{P}) \tag{2.37a}$$

$$\boldsymbol{A}^\dagger \coloneqq \frac{1}{\sqrt{2m\omega\hbar}} (m\omega \boldsymbol{Q} - \imath \boldsymbol{P}) . \tag{2.37b}$$

From the commutation relation 2.35 follows that the commutator of this operators is given by:

$$\left[\boldsymbol{A}, \boldsymbol{A}^\dagger\right] = 1 , \tag{2.38}$$

and the Hamiltonian 2.36 can be expressed in terms of this operators as

$$\boldsymbol{H} = \frac{1}{2} \hbar\omega \left(\boldsymbol{A}\boldsymbol{A}^\dagger + \boldsymbol{A}^\dagger \boldsymbol{A}\right) . \tag{2.39}$$

Creation and annihilation operators are not observable operators. In order to describe their physical meaning it is useful to investigate the effect that they have when applied to the Hamiltonian $\boldsymbol{H}$. Suppose that $\boldsymbol{H}$ diagonalizes respect to the complete basis $\{|n\rangle\}_n$ of the state space $\mathcal{H}$, i.e.,

$$\boldsymbol{H}|n\rangle = E_n |n\rangle . \tag{2.40}$$

From the equation 2.39 results

$$\boldsymbol{A}^\dagger \boldsymbol{H} = \frac{1}{2} \hbar\omega \left(\boldsymbol{A}^\dagger \boldsymbol{A}\boldsymbol{A}^\dagger + \boldsymbol{A}^\dagger \boldsymbol{A}^\dagger \boldsymbol{A}\right) \tag{2.41}$$

and using the commutation relation 2.38 on the first term of 2.41, it can be written as

$$\boldsymbol{A}^\dagger \boldsymbol{H} = \frac{1}{2} \hbar\omega \left(\boldsymbol{A}\boldsymbol{A}^\dagger \boldsymbol{A}^\dagger - \boldsymbol{A}^\dagger + \boldsymbol{A}^\dagger \boldsymbol{A}^\dagger \boldsymbol{A}\right) \tag{2.42a}$$

$$= \left[\hbar\omega \left(\boldsymbol{A}^\dagger \boldsymbol{A} + \frac{1}{2}\right)\right] \boldsymbol{A}^\dagger - \hbar\omega \boldsymbol{A}^\dagger \tag{2.42b}$$

$$= (\boldsymbol{H} - \hbar\omega)\ \boldsymbol{A}^\dagger . \tag{2.42c}$$

Let's then apply the creation operator on both sides of the equation 2.40:

$$\boldsymbol{A}^\dagger \boldsymbol{H} |n\rangle = \boldsymbol{A}^\dagger E_n |n\rangle \tag{2.43a}$$

$$(\boldsymbol{H} - \hbar\omega)\ \boldsymbol{A}^\dagger |n\rangle = E_n \boldsymbol{A}^\dagger |n\rangle \tag{2.43b}$$

$$\boldsymbol{H}\ \left(\boldsymbol{A}^\dagger |n\rangle\right) = (E_n + \hbar\omega)\ \left(\boldsymbol{A}^\dagger |n\rangle\right)\ . \tag{2.43c}$$

The state $\boldsymbol{A}^\dagger |n\rangle$ is therefore an eigenstate of the Hamiltonian $\boldsymbol{H}$ with eigenenergy $(E_n + \hbar\omega)$ and then: *the creation operator effect on the system is to bring it at an higher energy level.* Since $|n+1\rangle$ is the eigenstate of $\boldsymbol{H}$ associated to the eigenvalue $E_{n+1} = E_n + \hbar\omega$, the effect of the creation operator acting to $|n\rangle$ is to bring the system in the state $|n+1\rangle$:

$$\boldsymbol{A}^\dagger |n\rangle = c_n |n+1\rangle\ . \tag{2.44}$$

In a similar way the annihilation operator effect is to bring a SHO in the state $|n\rangle$ to the lower energy state $|n-1\rangle$ if $n > 1$ and to result 0 if $n = 0$:

$$\boldsymbol{A} |n\rangle = d_n |n-1\rangle \qquad \text{if} \quad n > 1 \tag{2.45a}$$

$$\boldsymbol{A} |0\rangle = 0 \qquad \text{if} \quad n = 0\,. \tag{2.45b}$$

The coefficients c_n and d_n can be obtained from the condition $\langle n|n\rangle = \langle n+1|n+1\rangle = 1$ and result

$$\boldsymbol{A}^\dagger |n\rangle = \sqrt{n+1}\, |n+1\rangle \tag{2.46a}$$

$$\boldsymbol{A} |n\rangle = \sqrt{n}\, |n-1\rangle\ . \tag{2.46b}$$

The states $|n\rangle$ are called **number states** or **Fock states** and the **number operator** $\boldsymbol{N} \coloneqq \boldsymbol{A}^\dagger \boldsymbol{A}$ is the quantum operator associated to the observable n, i.e.,

$$\boldsymbol{N} |n\rangle = n |n\rangle\ . \tag{2.47}$$

The state $|0\rangle$ is called **ground state** and represents the state of a SHO with the lowest admitted energy. Note that the ground state has not energy equal to 0 but its energy is given by:

$$\boldsymbol{H} |0\rangle = \hbar\omega \left(\boldsymbol{A}\,\boldsymbol{A}^\dagger + \frac{1}{2}\right) |0\rangle \tag{2.48a}$$

$$= \frac{\hbar\omega}{2} |0\rangle \tag{2.48b}$$

and is then equal to $E_0 = \hbar\omega/2$. Considering that the energy gap between two consecutive Fock states is $\hbar\omega$, the n-th energy level E_n then can be calculated and results $E_n = \left(n + \frac{1}{2}\right) \hbar\omega$.

Let's finally define a dimensionless form of position and momentum operators used in the initial expression 2.37 for the harmonic-oscillator Hamiltonian: the **quadrature operators** defined as:

$$\boldsymbol{X_1} = \sqrt{\frac{m\,\omega}{2\,\hbar}}\, \boldsymbol{Q} = \frac{1}{2}\ \left(\boldsymbol{A}^\dagger + \boldsymbol{A}\right) \tag{2.49a}$$

$$\boldsymbol{X_2} = \sqrt{\frac{1}{2\,m\,\hbar\,\omega}}\, \boldsymbol{P} = \frac{\imath}{2}\ \left(\boldsymbol{A}^\dagger - \boldsymbol{A}\right)\ . \tag{2.49b}$$

The quadrature operators are observables of the SHO, they satisfy the commutation relation

$$[\boldsymbol{X_1},\, \boldsymbol{X_2}] = \frac{\imath}{4} \tag{2.50}$$

and then their Heisenberg limit is

$$\Delta\boldsymbol{X_1}\, \Delta\boldsymbol{X_2} \geq \frac{1}{4}\,. \tag{2.51}$$

These operators are useful for the characterization of a SHO and they will be used for the description of some electromagnetic radiation quantum states.

2.2.3 Quantum description of the electromagnetic radiation

Electric and magnetic fields operators can be found looking that the Hamiltonian of the radiation 2.30 is formally identical to the SHO Hamiltonian 2.39 replacing the quantities $a_{\boldsymbol{k},\,\sigma}$ and $a^*_{\boldsymbol{k},\,\sigma}$ with the operators $\boldsymbol{A}_{\boldsymbol{k},\,\sigma}$ and $\boldsymbol{A}^\dagger_{\boldsymbol{k},\,\sigma}$ and setting

$$\frac{1}{2}\,\hbar\,\omega_{\boldsymbol{k}} = \epsilon_0\,A^2_{\boldsymbol{k}}\,\omega^2_{\boldsymbol{k}}\,V\,. \tag{2.52}$$

The equation 2.52 requires that the amplitude $A_{\boldsymbol{k}}$ is

$$A_{\boldsymbol{k}} = \sqrt{\frac{\hbar}{2\,\epsilon_0\,V\,\omega_{\boldsymbol{k}}}}\,. \tag{2.53}$$

The field's Hamiltonian operator results

$$\boldsymbol{H} = \sum_{\boldsymbol{k},\,\sigma} \hbar\,\omega_{\boldsymbol{k}}\,\left[\boldsymbol{A}_{\boldsymbol{k},\,\sigma}\,\boldsymbol{A}^\dagger_{\boldsymbol{k},\,\sigma} + \frac{1}{2}\right]\,, \tag{2.54}$$

with $\boldsymbol{A}_{\boldsymbol{k},\,\sigma}$ and $\boldsymbol{A}^\dagger_{\boldsymbol{k},\,\sigma}$ that satisfy the following relations:

$$\left[\boldsymbol{A}_{\boldsymbol{k},\,\sigma},\,\boldsymbol{A}^\dagger_{\boldsymbol{k'},\,\sigma'}\right] = \delta_{\boldsymbol{k},\,\boldsymbol{k'}}\,\delta_{\sigma,\,\sigma'} \tag{2.55a}$$

$$\left[\boldsymbol{A}_{\boldsymbol{k},\,\sigma},\,\boldsymbol{A}_{\boldsymbol{k'},\,\sigma'}\right] = 0 \tag{2.55b}$$

$$\left[\boldsymbol{A}^\dagger_{\boldsymbol{k},\,\sigma},\,\boldsymbol{A}^\dagger_{\boldsymbol{k'},\,\sigma'}\right] = 0\,. \tag{2.55c}$$

The field operators $\boldsymbol{E}$ and $\boldsymbol{B}$ can be obtained from the equations 2.29 in the same way of the Hamiltonian and result

$$\boldsymbol{E} = \sum_{\boldsymbol{k},\,\sigma} \sqrt{\frac{\hbar\,\omega_{\boldsymbol{k}}}{2\,\epsilon_0\,V}}\,\imath\,\hat{\boldsymbol{e}}_{\boldsymbol{k},\,\sigma}\left(\boldsymbol{A}_{\boldsymbol{k},\,\sigma}\,e^{\imath\,\boldsymbol{k}\cdot\boldsymbol{r}} - \boldsymbol{A}^\dagger_{\boldsymbol{k},\,\sigma}\,e^{-\imath\,\boldsymbol{k}\cdot\boldsymbol{r}}\right) \tag{2.56a}$$

$$\boldsymbol{B} = \sum_{\boldsymbol{k},\,\sigma} \sqrt{\frac{\hbar}{2\,\epsilon_0\,\omega_{\boldsymbol{k}}\,V}}\,\imath\,\boldsymbol{k}\times\hat{\boldsymbol{e}}_{\boldsymbol{k},\,\sigma}\left(\boldsymbol{A}_{\boldsymbol{k},\,\sigma}\,e^{\imath\,\boldsymbol{k}\cdot\boldsymbol{r}} - \boldsymbol{A}^\dagger_{\boldsymbol{k},\,\sigma}\,e^{-\imath\,\boldsymbol{k}\cdot\boldsymbol{r}}\right)\,. \tag{2.56b}$$

We highlight that both operator are time-indipendent due to the choice of use the Schrodinger's picture of QM but they are position-dependent. The dipendency is omitted in order to simplify the notation.

2.2.4 Single mode electromagnetic radiation

Previous sections show that the electromagnetic radiation is an observable quantity that can be measured in a photons system. Considering now a radiation with only one propagation mode, this section investigates the properties of some useful and well-known photon systems. During all the following discussion the subsriptions $\boldsymbol{k}$ and σ are omitted due to the fact that a single mode radiation is considered. This assumption involves that the radiation consists of indistinguishable photons and can completely described as a SHO.

Fock states

Fock states $|n\rangle$ (or number states) are a complete basis for single single-mode states and they are so the natural starting point for a treatment of single-mode light. Instead of the simply meaning of the number states, it is very hard to generate experimentally a light in these states.

The first interesting property of a single-mode radiation is the **photon number distribution** that consists in the probability density function (PDF) of the measurement of the photon

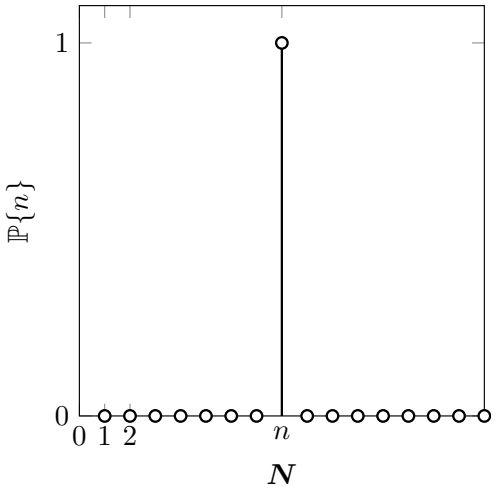

(a) Photon number distribution of a Fock state.

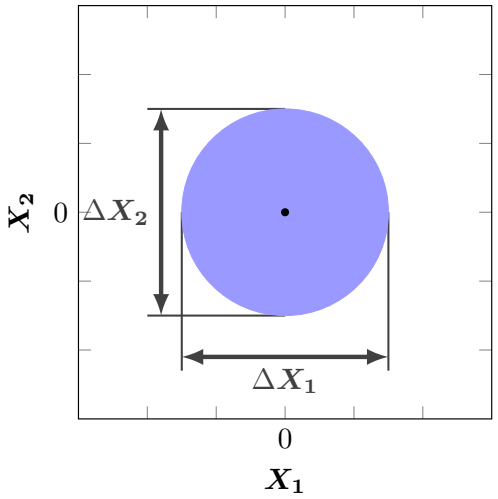

(b) Phase state representation of a number state.

Figure 2.1: Number state $|n\rangle$ photon number distribution and phase-space representation.

number (observable $\boldsymbol{N}$). Expected value and variance of the number of photons can be obtained using the equation 2.47 and result

$$\begin{aligned}
\langle \boldsymbol{N} \rangle &= \langle n | \, \boldsymbol{N} \, | n \rangle && \text{(2.57a)} \\
&= n \, \langle n | n \rangle = n && \text{(2.57b)} \\
\langle (\Delta \boldsymbol{N})^2 \rangle &= \langle \boldsymbol{N}^2 \rangle - \langle \boldsymbol{N} \rangle^2 && \text{(2.57c)} \\
&= \langle n | \, \boldsymbol{N} \, \boldsymbol{N} \, | n \rangle - n^2 && \text{(2.57d)} \\
&= n^2 - n^2 = 0 \, . && \text{(2.57e)}
\end{aligned}$$

The photon number distribution of the Fock state $|n\rangle$ is then a discrete impulsive distribution as shown in the figure 2.1a.

It is also possible to describe the state by means of the quadrature operators outcomes exected values and variances (**phase-space characterization**). More sophisticated analysis consists in the definition of quasi-probability functions that aim to describe the quadrature operators outcomes PDF. In this context the derivation of the expected values and variances and their time-evolution are described. The time evolution of a state is obtained from the Schrödinger equation and for Fock states results:

$$\begin{aligned}
\imath \hbar \frac{\partial \, |n(t)\rangle}{\partial t} &= \boldsymbol{H} \, |n(t)\rangle = \hbar \omega \left(\frac{1}{2} + n \right) \, |n(t)\rangle && \text{(2.58a)} \\
|n(t)\rangle &= e^{-\imath \omega \left(\frac{1}{2} + n \right) t} \, |n(0)\rangle = e^{-\imath \omega \left(\frac{1}{2} + n \right) t} \, |n\rangle \, . && \text{(2.58b)}
\end{aligned}$$

Observing that

$$\begin{aligned}
\boldsymbol{A} \, |n(t)\rangle &= e^{-\imath \omega \left(\frac{1}{2} + n \right) t} \, \boldsymbol{A} \, |n\rangle && \text{(2.59a)} \\
&= e^{-\imath \omega t} \, e^{-\imath \omega \left(\frac{1}{2} + n - 1 \right) t} \, \sqrt{n} \, |n-1\rangle && \text{(2.59b)} \\
&= \sqrt{n} e^{-\imath \omega t} \, |[n-1]\,(t)\rangle && \text{(2.59c)} \\
\boldsymbol{A} \, |n(t)\rangle^\dagger &= \sqrt{n+1} \, e^{\imath \omega t} \, |[n+1]\,(t)\rangle \, , && \text{(2.59d)}
\end{aligned}$$

the expected values of quadrature operators result

$$\langle \boldsymbol{X_1} \rangle = \langle n(t)| \boldsymbol{X_1} |n(t)\rangle \tag{2.60a}$$
$$= \frac{1}{2} \langle n(t)| \left(\boldsymbol{A} + \boldsymbol{A}^\dagger\right) |n(t)\rangle \tag{2.60b}$$
$$= \frac{1}{2} \left(\sqrt{n}\, e^{-\imath\,\omega\,t} \langle n|n-1\rangle + \sqrt{n+1}\, e^{\imath\,\omega\,t} \langle n|n+1\rangle\right) = 0 \tag{2.60c}$$
$$\langle \boldsymbol{X_2} \rangle = \langle n(t)| \boldsymbol{X_2} |n(t)\rangle \tag{2.60d}$$
$$= \frac{1}{2} \langle n(t)| \left(\boldsymbol{A} - \boldsymbol{A}^\dagger\right) |n(t)\rangle = 0, \tag{2.60e}$$

and the variances are given by

$$\langle (\Delta \boldsymbol{X_1})^2 \rangle = \langle \boldsymbol{X_1^2} \rangle - \langle \boldsymbol{X_1} \rangle^2 \tag{2.61a}$$
$$= \frac{1}{4} \langle n(t)| \left(\boldsymbol{A}\boldsymbol{A} + \boldsymbol{A}^\dagger\boldsymbol{A}^\dagger + \boldsymbol{A}^\dagger\boldsymbol{A} + \boldsymbol{A}\boldsymbol{A}^\dagger\right) |n(t)\rangle - 0 \tag{2.61b}$$
$$= \frac{1}{4} (n + n + 1) = \frac{1}{2} \left(n + \frac{1}{2}\right) \tag{2.61c}$$
$$\langle (\Delta \boldsymbol{X_2})^2 \rangle = \langle \boldsymbol{X_2^2} \rangle - \langle \boldsymbol{X_2} \rangle^2 \tag{2.61d}$$
$$= \frac{1}{2} \left(n + \frac{1}{2}\right). \tag{2.61e}$$

We can notice that the Heisnberg bound is respected:

$$\Delta \boldsymbol{X_1}\, \Delta \boldsymbol{X_2} = \frac{1}{2} \left(n + \frac{1}{2}\right) \geq \frac{1}{4}. \tag{2.62}$$

It is possible to plot in a plane the phase-space representation of the state as we can see in figure 2.1b. In the axis we have the possible outcomes of quadrature observables measurements and the representation simply shows the space region described by the outcomes expected value $\langle \boldsymbol{X_i} \rangle$ and variance $\langle (\Delta \boldsymbol{X_i})^2 \rangle$. For a number state, the phase-space representation is a circle with radius $\frac{1}{2}\left(n + \frac{1}{2}\right)$ and zero-centered. The minimum-variance state is the vacuum state $|0\rangle$ with variance 1/4.

Finally, it is interesting to find expected value and variance of the electric field of a Fock photon state since it is one of the only two observables associated to the electromagnetic radiation by classical mechanics (together with the magnetic field). The electric field mean is given (using the electric field operator 2.56) by the following expression assuming that the propagation is only in direction z, i.e., $\boldsymbol{k} = k_z\, \hat{\boldsymbol{z}} = k\, \hat{\boldsymbol{z}}$:

$$\langle n(t)| \boldsymbol{E} |n(t)\rangle = \sqrt{\frac{\hbar\,\omega}{2\,\epsilon_0\,V}}\, \imath \hat{\boldsymbol{e}} \left(\langle n(t)| \boldsymbol{A} |n(t)\rangle\, e^{\imath\, k\, z} - \langle n(t)| \boldsymbol{A}^\dagger |n(t)\rangle\, e^{-\imath\, k\, z}\right) = 0. \tag{2.63}$$

The electric field variance is given by:

$$\langle n(t)| (\Delta \boldsymbol{E})^2 |n(t)\rangle = \langle n(t)| \boldsymbol{E} \cdot \boldsymbol{E} |n(t)\rangle - \left(\langle n(t)| \boldsymbol{E} |n(t)\rangle\right)^2 \tag{2.64a}$$
$$= \langle n(t)| - \frac{\hbar\,\omega}{2\,\epsilon_0\,V} \left(\boldsymbol{A}^2\, e^{\imath\, 2\, k\, z} + \boldsymbol{A}^{\dagger 2}\, e^{-\imath\, 2\, k\, z} - 2\, \boldsymbol{A}^\dagger\, \boldsymbol{A} - 1\right) |n(t)\rangle \tag{2.64b}$$
$$= \frac{\hbar\,\omega}{\epsilon_0\,V} \left(n + \frac{1}{2}\right). \tag{2.64c}$$

Observe that the electric-field variance is time-indipendent. In the figure 2.2 is plotted the field as a function of time t. The black line represents the mean of the field and the blue region is the region described by the deviation $\Delta \boldsymbol{E}$.

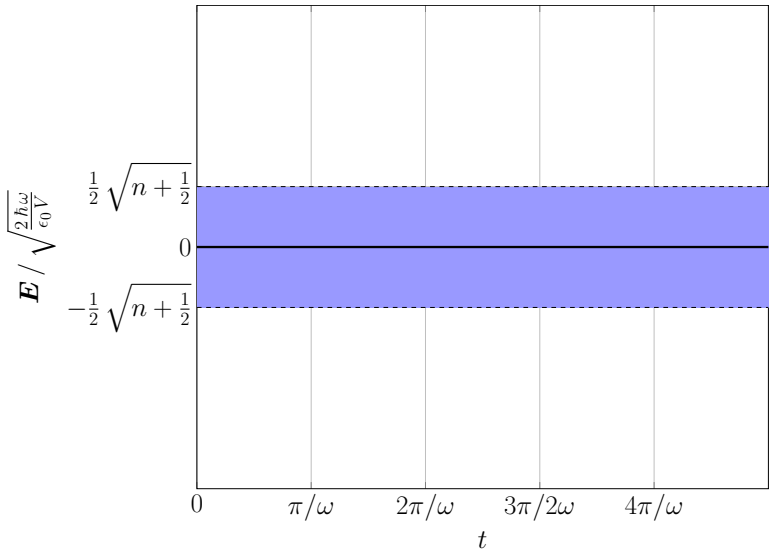

Figure 2.2: Representation of the normalized electric field of a Fock state.

Coherent states

A coherent state is the most classical quantum state of radiation. Differently from number states, it can be simply generated with an ideal laser beam.

A coherent state $|\mu\rangle$ is defined as the eigenstate of the annihilation operator:

$$\boldsymbol{A}\,|\mu\rangle = \mu\,|\mu\rangle\ . \tag{2.65}$$

The photon number statistic of a coherent state can be obtained from the definition 2.65 expanding the state $|\mu\rangle$ in number-states basis:

$$|\mu\rangle = \sum_{n=0}^{+\infty} c_n\,|n\rangle\ . \tag{2.66}$$

Replacing the expression 2.66 into the equation 2.65, results

$$\sum_{n=0}^{+\infty} c_n\,\mu\,|n\rangle = \sum_{n=0}^{+\infty} c_n\,\boldsymbol{A}\,|n\rangle \tag{2.67a}$$

$$= \sum_{n=1}^{+\infty} c_n\,\sqrt{n}\,|n-1\rangle \tag{2.67b}$$

$$= \sum_{n=0}^{+\infty} c_{n+1}\,\sqrt{n+1}\,|n\rangle\ . \tag{2.67c}$$

Expanding the recurrency relation between the coefficients c_n, is possible to find their expression as it follows:

$$c_n = \frac{\mu}{\sqrt{n}}\,c_{n-1} = \cdots = \frac{\mu^n}{\sqrt{n!}}\,c_0 \tag{2.68}$$

where c_0 can be obtained expliting the unitary norm condition

$$1 = \langle\mu|\mu\rangle = \sum_{n=0}^{+\infty}\sum_{m=0}^{+\infty} |c_0|^2\,\frac{(\mu^*)^m\,\mu^n}{\sqrt{n!\,m!}}\,\langle m|n\rangle \tag{2.69a}$$

$$= \sum_{n=0}^{+\infty} |c_0|^2\,\frac{|\mu|^{2\,n}}{n!} = |c_0|^2\,e^{|\mu|^2}\ . \tag{2.69b}$$

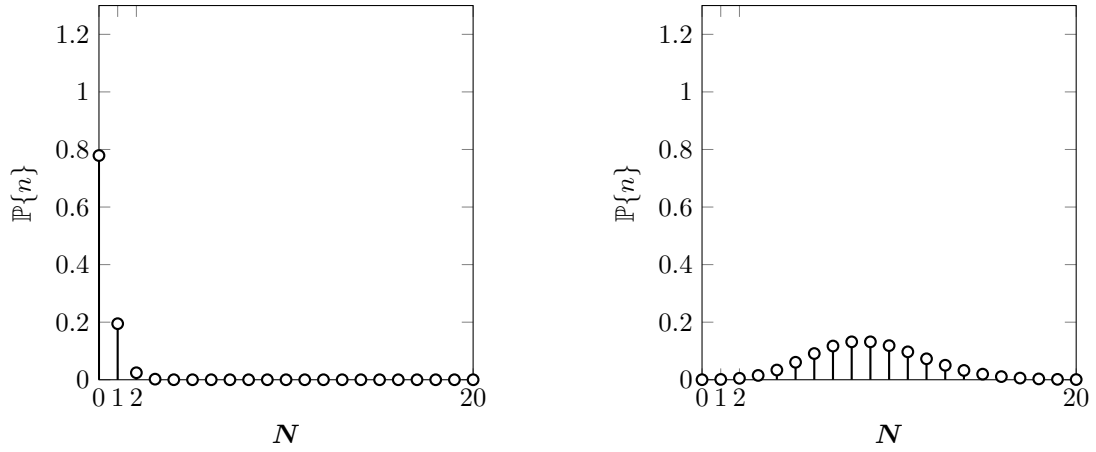

(a) $|\mu| = 0.5$ (b) $|\mu| = 3$

Figure 2.3: Photon distribution for a coherent state $|\mu\rangle$.

It follows that

$$c_0 = e^{-\frac{|\mu|^2}{2}} \tag{2.70}$$

and that the coherent state can be expanded as

$$|\mu\rangle = e^{-\frac{|\mu|^2}{2}} \sum_{n=0}^{+\infty} \frac{\mu^n}{\sqrt{n!}} |n\rangle \ . \tag{2.71}$$

The time evolution of a coherent state can be found (as for the number states) from the Schrödinger's equation and results

$$|\mu(t)\rangle = e^{-\frac{|\mu|^2}{2}} \sum_{n=0}^{+\infty} \frac{\mu^n}{\sqrt{n!}} e^{-\imath\,\omega\left(\frac{1}{2}+n\right)t} |n\rangle \ . \tag{2.72}$$

Observe that

$$\boldsymbol{A}\,|\mu(t)\rangle = \mu\, e^{-\imath\,\omega\,t}\ |\mu(t)\rangle \tag{2.73a}$$

$$\langle\mu(t)|\,\boldsymbol{A}^\dagger = \langle\mu(t)|\,\mu^*\, e^{\imath\,\omega\,t}\,. \tag{2.73b}$$

The photon distribution can be calculated as

$$\mathbb{P}\{n\} = |\langle n(t)|\mu(t)\rangle|^2 = e^{-|\mu|^2}\ \frac{|\mu|^{2n}}{n!} \tag{2.74}$$

and results time-invariant. The photon number expected value and variance are

$$\langle\boldsymbol{N}\rangle = \langle\mu(t)|\,\boldsymbol{N}\,|\mu(t)\rangle = \langle\mu(t)|\,\boldsymbol{A}^\dagger\boldsymbol{A}\,|\mu(t)\rangle \tag{2.75a}$$

$$= |\mu|^2\ \langle\mu(t)|\mu(t)\rangle = |\mu|^2 \tag{2.75b}$$

$$\langle(\Delta\boldsymbol{N})^2\rangle = \langle\mu(t)|\,\boldsymbol{N}^2\,|\mu(t)\rangle - \langle\boldsymbol{N}\rangle^2 \tag{2.75c}$$

$$= \langle\boldsymbol{N}\rangle = |\mu|^2\,. \tag{2.75d}$$

In figure 2.3 are plotted the photon number distributions of a coherent state for different values of μ.

In order to provide a phase-space representation for a coherent state $|\mu(t)\rangle$, let's start with the calculus of mean and variance of the quadrature operators. The mean values $\langle\boldsymbol{X_1}\rangle$ and

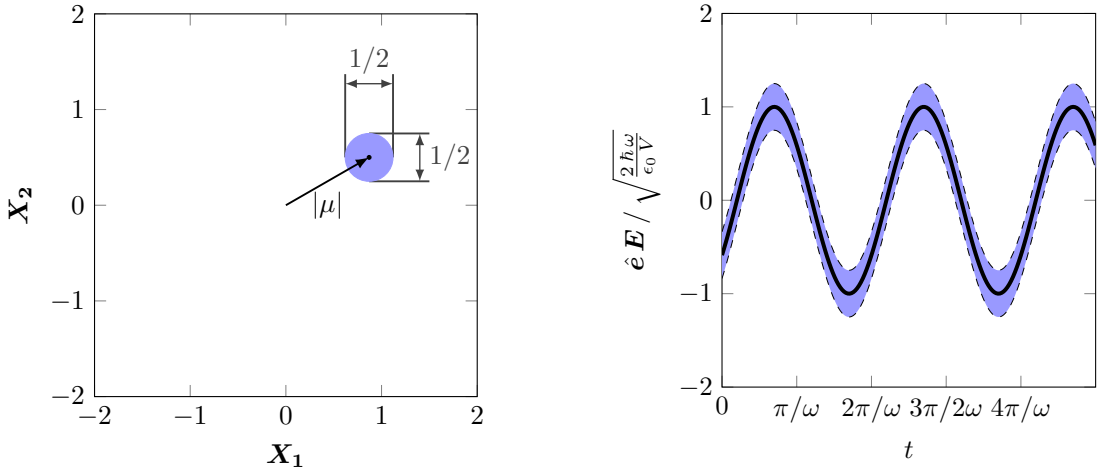

(a) Phase-space representation

(b) Time evolution of the electric field for a fixed position z.

Figure 2.4: Phase-space and electric field representations for a coherent state $|\mu\rangle$.

$\langle \boldsymbol{X_2} \rangle$ are given by:

$$\langle \boldsymbol{X_1} \rangle = \langle \mu(t)| \boldsymbol{X_1} |\mu(t)\rangle = \frac{1}{2} \langle \mu(t)| \left(\boldsymbol{A} + \boldsymbol{A}^\dagger\right) |\mu(t)\rangle \tag{2.76a}$$

$$= \frac{1}{2} \left(\mu\, e^{-\imath\,\omega\,t} + \mu^*\, e^{\imath\,\omega\,t}\right) \tag{2.76b}$$

$$\langle \boldsymbol{X_2} \rangle = \langle \mu(t)| \boldsymbol{X_2} |\mu(t)\rangle = \frac{1}{2\imath} \langle \mu(t)| \left(\boldsymbol{A} - \boldsymbol{A}^\dagger\right) |\mu(t)\rangle \tag{2.76c}$$

$$= \frac{1}{2\imath} \left(\mu\, e^{-\imath\,\omega\,t} - \mu^*\, e^{\imath\,\omega\,t}\right), \tag{2.76d}$$

and the variances result

$$\langle (\Delta \boldsymbol{X_1})^2 \rangle = \langle \mu(t)| \boldsymbol{X_1}^2 |\mu(t)\rangle - \langle \mu(t)| \boldsymbol{X_1} |\mu(t)\rangle^2 \tag{2.77a}$$

$$= \frac{1}{4} \langle \mu(t)| \left(\boldsymbol{A}^2 + \left(\boldsymbol{A}^\dagger\right)^2 + \boldsymbol{A}\boldsymbol{A}^\dagger + \boldsymbol{A}^\dagger\boldsymbol{A}\right) |\mu(t)\rangle - \langle \boldsymbol{X_1} \rangle^2 = \frac{1}{4}, \tag{2.77b}$$

$$\langle (\Delta \boldsymbol{X_2})^2 \rangle = \langle \mu(t)| \boldsymbol{X_2}^2 |\mu(t)\rangle - \langle \mu(t)| \boldsymbol{X_2} |\mu(t)\rangle^2 \tag{2.77c}$$

$$= -\frac{1}{4} \langle \mu(t)| \left(\boldsymbol{A}^2 + \left(\boldsymbol{A}^\dagger\right)^2 - \boldsymbol{A}\boldsymbol{A}^\dagger - \boldsymbol{A}^\dagger\boldsymbol{A}\right) |\mu(t)\rangle - \langle \boldsymbol{X_1} \rangle^2 = \frac{1}{4}. \tag{2.77d}$$

As it is shown in figure 2.4a a coherent state looks like a circle with radius 1/2 (deviation) and center on a circonference with radius $|\mu|$ in the phase-diagram. The time-evolution of the state moves the circle around the μ-radius circonference.

Finally, observe that variance of the state for every μ value is 1/4 as for the vacuum state $|0\rangle$. Form this observation follows that we can describe a coherent state as the vacuum state "shifted" of μ in the phase-space. This interpretation can be represented mathematically with the **choerent-state displacement operator** ($\boldsymbol{D}_\mu$). The expression of $\boldsymbol{D}_\mu$ in terms of annihilation and creation operator can be found from the fock representation of the coherent state 2.71 as it follows

$$|\mu\rangle = e^{-\frac{|\mu|^2}{2}} \sum_{n=0}^{+\infty} \frac{\mu^n}{\sqrt{n!}} |n\rangle = e^{-\frac{|\mu|^2}{2}} \sum_{n=0}^{+\infty} \frac{\left(\mu\, \boldsymbol{A}^\dagger\right)^n}{\sqrt{n!}} |0\rangle \tag{2.78a}$$

$$= e^{\mu\, \boldsymbol{A}^\dagger - \frac{1}{2}|\mu|^2} |0\rangle = \boldsymbol{D}_\mu |0\rangle \tag{2.78b}$$

and rewriting it in the following form

$$\boldsymbol{D}_\mu = e^{\mu\, \boldsymbol{A}^\dagger - \mu^*\, \boldsymbol{A}}. \tag{2.79}$$

It is easy to show that the displacement operator is unitary, i.e $\boldsymbol{D}_\mu^\dagger \boldsymbol{D}_\mu = \boldsymbol{D}_\mu \boldsymbol{D}_\mu^\dagger = \boldsymbol{I}$, and

$$\boldsymbol{D}_\mu^\dagger \, \boldsymbol{A} \, \boldsymbol{D}_\mu = \boldsymbol{A} + \mu \tag{2.80a}$$

$$\boldsymbol{D}_\mu \, \boldsymbol{A}^\dagger \, \boldsymbol{D}_\mu^\dagger = \boldsymbol{A}^\dagger + \mu^* \, . \tag{2.80b}$$

The electric field associated to a photons coherent-state can be finally calculated. The mean of the field $\langle \boldsymbol{E} \rangle$ is given by

$$\langle \boldsymbol{E} \rangle = \langle \mu(t) | \, \boldsymbol{E} \, | \mu(t) \rangle = \sqrt{\frac{\hbar\,\omega}{2\,\epsilon_0\,V}} \, \imath \hat{\boldsymbol{e}} \left(\langle \mu(t) | \, \boldsymbol{A} \, | \mu(t) \rangle \; e^{-\imath\, k\, z} - \langle \mu(t) | \, \boldsymbol{A}^\dagger \, | \mu(t) \rangle \; e^{\imath\, k\, z} \right) \tag{2.81a}$$

$$= -\sqrt{\frac{\hbar\,\omega}{2\,\epsilon_0\,V}} \, \imath \hat{\boldsymbol{e}} \left(\mu \, e^{-\imath\,(\omega\, t + k\, z)} - \mu^* \, e^{\imath\,(\omega\, t + k\, z)} \right) \tag{2.81b}$$

$$= \hat{\boldsymbol{e}} \sqrt{\frac{2\,\hbar\,\omega}{\epsilon_0\,V}} \, |\mu| \, \sin\left[\omega\, t + k\, z - \arg(\mu)\right] \tag{2.81c}$$

and it is possible to observe that the electric field mean is similar to a classical single-mode electric field expression. However, differently from the classical physics vision, now we have a variance of the field given by

$$\left\langle (\Delta \boldsymbol{E})^2 \right\rangle = \langle \mu(t) | \, (\Delta \boldsymbol{E})^2 \, | \mu(t) \rangle = \langle \mu(t) | \, (\boldsymbol{E} \cdot \boldsymbol{E}) \, | \mu(t) \rangle - \langle \boldsymbol{E} \rangle^2 \tag{2.82a}$$

$$= -\frac{\hbar\,\omega}{2\,\epsilon_0\,V} \, \langle \mu(t) | \left(\boldsymbol{A}^2 \, e^{-\imath\, 2k\, z} + \left(\boldsymbol{A}^\dagger \right)^2 \, e^{\imath\, 2k\, z} - 2\boldsymbol{A}^\dagger \boldsymbol{A} - 1 \right) | \mu(t) \rangle - \langle \boldsymbol{E} \rangle^2 \tag{2.82b}$$

$$= -\frac{\hbar\,\omega}{2\,\epsilon_0\,V} \left(\mu^2 \, e^{-\imath\,(2\omega\, t - 2k\, z)} + (\mu^*)^2 \, e^{+\imath\,(2\omega\, t - 2k\, z)} - 2|\mu|^2 - 1 \right) - \langle \boldsymbol{E} \rangle^2 \tag{2.82c}$$

$$= \frac{\hbar\,\omega}{2\,\epsilon_0\,V} \, . \tag{2.82d}$$

Figure 2.4b plot the electric field and its variance. The black line is the mean of the field and it is similar to a classic field with the same properties. The blue region are values of field descrived by the deviation $\langle \Delta \boldsymbol{E} \rangle$. Note that the variance is time-indipendent.

Squeezed vacuum state

The states that we have described in the last pages have a common property: the quadrature-operator variances are identical. It is possible to define an operator $\boldsymbol{S}_\zeta$ that modifies the variances $\Delta \boldsymbol{X_i}$: the **squeezing operator**. The single-mode quadrature-squeezed vacuum state defined as

$$|\zeta\rangle \coloneqq \boldsymbol{S}_\zeta \, |0\rangle \tag{2.83}$$

and has $\Delta \boldsymbol{X_1} \neq \Delta \boldsymbol{X_2}$. Despite this, the Heisenberg bound is always satisfied, i.e., $\Delta \boldsymbol{X_1} \, \Delta \boldsymbol{X_2} \geq 1/4$. Squeezed states do not have any classical analogues and they are used in a lot of high-precision interferometry like the gravitational-wave LIGO interferometer [33].

The single-mode squeezing operator is defined as

$$\boldsymbol{S}_\zeta \coloneqq e^{\frac{1}{2}\left(\zeta^* \left(\boldsymbol{A}^\dagger \right)^2 - \zeta \boldsymbol{A}^2 \right)} \tag{2.84}$$

and satisfies the unitary condition $\boldsymbol{S}_\zeta^\dagger \boldsymbol{S}_\zeta = \boldsymbol{S}_\zeta \boldsymbol{S}_\zeta^\dagger = \boldsymbol{I}$. The parameter ζ is a complex number, it can be expressed as $\zeta = r \, e^{\imath\,\theta}$, and it satisfies following relations:

$$\boldsymbol{S}_\zeta^\dagger \, \boldsymbol{A} \, \boldsymbol{S}_\zeta = \boldsymbol{A} \cosh r - \boldsymbol{A}^\dagger \, e^{\imath\,\theta} \sinh r \tag{2.85a}$$

$$\boldsymbol{S}_\zeta^\dagger \, \boldsymbol{A}^\dagger \, \boldsymbol{S}_\zeta = \boldsymbol{A}^\dagger \cosh r - \boldsymbol{A} \, e^{-\imath\,\theta} \sinh r \, . \tag{2.85b}$$

The Fock representation of vacuum-squeezed states can be obtained as for the coherent states and results

$$|\zeta\rangle = (\operatorname{sech}(r))^{1/2} \sum_{n=0}^{+\infty} \frac{[(2n)!]^{1/2}}{n!} \left[-\frac{1}{2} e^{\imath\,\theta} \tanh(r) \right]^n \, |2n\rangle \; . \tag{2.86}$$

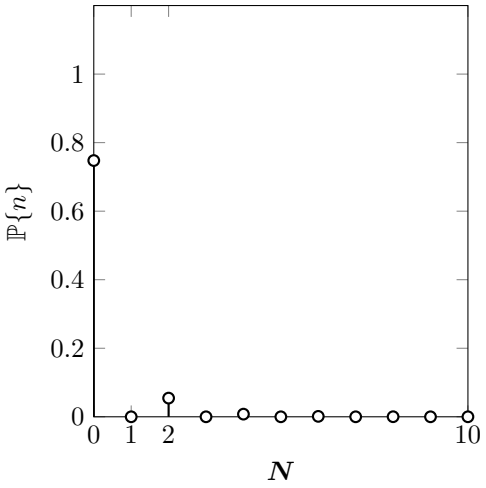

(a) Photon distribution of $|\zeta\rangle$ with $r = 0.8$ and $\theta = \pi$.

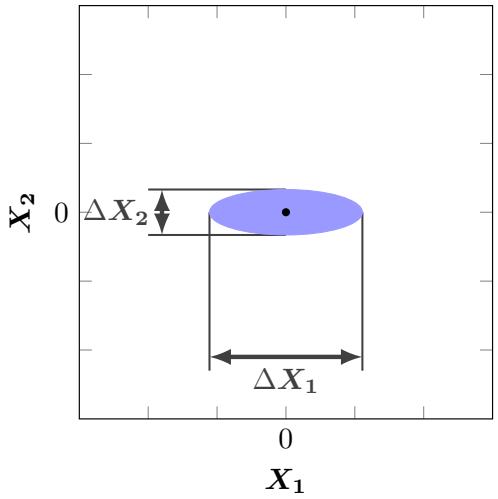

(b) Phase-space representation of the state $|\zeta\rangle$ with $r = 0.8$ and $\theta = \pi$.

Figure 2.5: Phase-space and electric field representations for a coherent state $|\mu\rangle$.

The time-evolution of the state can be calculated from the Schrodinger's equation and it is given by

$$|\zeta(t)\rangle = (\operatorname{sech}(r))^{1/2} \sum_{n=0}^{+\infty} \frac{[(2n)!]^{1/2}}{n!} \left[-\frac{1}{2} e^{\imath\,\theta} \tanh(r)\right]^n e^{-\imath\,\omega\left(\frac{1}{2}+2n\right)t} |2n\rangle \,. \tag{2.87}$$

The mean photon-number is given by $\langle \boldsymbol{N} \rangle$ and can be calculated considering the unitarity of the squeezing-operator as it follows

$$\begin{aligned} \langle \boldsymbol{N} \rangle &= \langle \zeta(t)| \boldsymbol{A}^\dagger \boldsymbol{A} |\zeta(t)\rangle && \text{(2.88a)} \\ &= \langle 0(t)| \boldsymbol{S}_\zeta^\dagger \boldsymbol{A}^\dagger \boldsymbol{S}_\zeta \boldsymbol{S}_\zeta^\dagger \boldsymbol{A} \boldsymbol{S}_\zeta |0(t)\rangle && \text{(2.88b)} \\ &= (\sinh(r))^2 \,. && \text{(2.88c)} \end{aligned}$$

The variance of $\boldsymbol{N}$ results

$$\langle (\Delta \boldsymbol{N})^2 \rangle = 2 \langle \boldsymbol{N} \rangle (\langle \boldsymbol{N} \rangle + 1) \,. \tag{2.89}$$

Figure 2.5a plots the photon number distribution previously described. From the equations 2.85 is possible to show that

$$\langle \zeta| \boldsymbol{X_1} |\zeta\rangle = \langle \zeta| \boldsymbol{X_2} |\zeta\rangle = 0 \,, \tag{2.90}$$

and that variances of the quadrature operators are

$$\langle (\Delta \boldsymbol{X_1})^2 \rangle = \frac{1}{4} \left\{ e^{2\,r} \left[\sin\left(\frac{1}{2}\theta\right)\right]^2 + e^{-2\,r} \left[\cos\left(\frac{1}{2}\theta\right)\right]^2 \right\} \tag{2.91a}$$

$$\langle (\Delta \boldsymbol{X_2})^2 \rangle = \frac{1}{4} \left\{ e^{2\,r} \left[\cos\left(\frac{1}{2}\theta\right)\right]^2 + e^{-2\,r} \left[\sin\left(\frac{1}{2}\theta\right)\right]^2 \right\} . \tag{2.91b}$$

In the figure 2.5b it is possible to observe that the ζ-parameter set the direction (θ) and the magnitude (r) of the squeezing in the phase-space. Despite this the Heisenberg uncertainty relation $\Delta \boldsymbol{X_1}\, \Delta \boldsymbol{X_2} \geq 1/2$ is always respected.

The electric field mean and variance can be computed. The results, normalized respect to

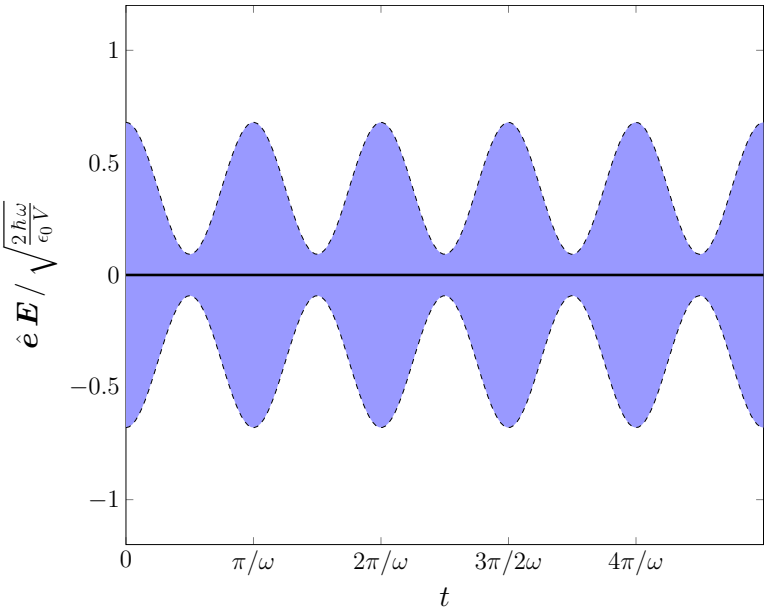

Figure 2.6: Time dependet normalized electric field amplitude associated to the squeezed vacuum state $|\zeta\rangle$ with $r = 0.5$ and $\theta = \pi$.

the constant $\sqrt{\frac{2\hbar\omega}{\epsilon_0 V}}$, are shown in the following lines:

$$\langle \boldsymbol{E} \rangle = \langle \zeta(t)| \boldsymbol{E} |\zeta(t)\rangle = 0 \tag{2.92a}$$

$$\langle (\Delta \boldsymbol{E})^2 \rangle = \frac{1}{4}\left\{ e^{2r}\left[\sin\left(\omega t - k z - \frac{1}{2}\theta\right)\right]^2 + e^{-2r}\left[\cos\left(\omega t - k z - \frac{1}{2}\theta\right)\right]^2 \right\} . \tag{2.92b}$$

In the figure 2.6 is plotted the field amplitude as a function of time (the position z is fixed). It is possible to observe that the electric field amplitude has zero mean but, differently to Fock states, the uncertainty is time and space dependent and has minimum points with values

$$\Delta \boldsymbol{E}_{\min} = \frac{1}{2} e^{-r} . \tag{2.93}$$

Squeezed coherent state

In the same way we obtain coherent states applying the displacement operator to the vacuum state, we can define the **squeezed coherent state** with displacement paramenter μ and squeezing parameter ζ as

$$|\mu, \zeta\rangle \coloneqq \boldsymbol{D}_\mu \boldsymbol{S}_\zeta |0\rangle . \tag{2.94}$$

Squeezed coherent states are identical to coherent states in the mean values but share with the squeezed vacuum state some properties about the quadrature observables uncertainty. It is possible to mathematically investigate the descriptions of such states as it was done for the previous states but it requires some sophisticated algebraic tools and it is not topic of this thesis to provide them. A more in-depth treatment can be found in [34].

Thermal state

The last photon state that we describe is the **thermal photon state**. In this paragraph is briefly described the photon distribution of an unexcited electromagnetic system in thermal equilibrium. The formulation is based on the Planck black-body work [21] and in particular on

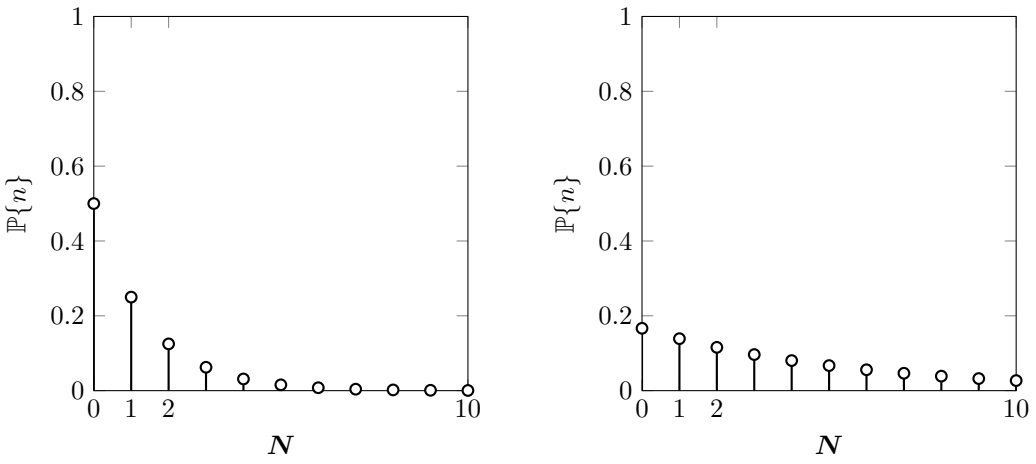

(a) $n_{\rm th} = 1$ (b) $n_{\rm th} = 5$

Figure 2.7: Photon number distributions of $\boldsymbol{\Xi}_{\rm th}$.

its definition of the mean number of thermal photons $n_{\rm th}$ for the mode of radiation with energy $E = \hbar\,\omega$:

$$n_{\rm th} = \frac{1}{\exp\{(\hbar\,\omega)/(k_{\rm B}\,T)\} - 1}\,, \tag{2.95}$$

where $k_{\rm B}$ is the Boltzmann's constant and T is the absolute temperature of the system. The single mode thermal state has Fock representation given by:

$$\boldsymbol{\Xi}_{\rm th} = \sum_n \frac{n_{\rm th}^n}{(1+n_{\rm th})^{1+n}}\ |n\rangle\langle n| \tag{2.96}$$

and then the probability that the measured observable $\boldsymbol{N}$ is equal to n results

$$\mathbb{P}\{n\} = {\rm tr}\{|n\rangle\langle n|\,\boldsymbol{\Xi}_{\rm th}\} = \frac{n_{\rm th}^n}{(1+n_{\rm th})^{1+n}}\,. \tag{2.97}$$

Figures 2.7 plot the photon number distributions of single-mode thermal states with some mean number of photons $n_{\rm th}$.

Chapter 3

Estimation and decision theory applied on quantum systems

In this chapter is described the application of estimation and decision theories on quantum systems. The capability to make decisions or estimate unknown parameters of systems is the foundation of many quantum and classical technologies. In this thesis the main goal is to provide the tools for understanding the QI protocol that will be described in the next chapter. Nevertheless, this chapter aims to provide an overall view of the topic due to its relevance in possible future developments.

As in classical systems the random nature of the environment requires the definition of strategies to infer an unknown parameter but, in addition, the randomness of quantum measurements contributes to complicate the estimation. The discussion is divided in two sections that correspond to the two macro-areas of the topic: the decision theory and the estimation theory.

3.1 Quantum decision theory

Decision theory is the tool that enables to make decisions between two or more hypotheses. The hypotheses may cover the value of a system parameter, a PDF of it or more generally a property of a system. Classical techniques involve the analysis of conditional PDFs in order to estabilish the best decision strategy. When the system is a quantum system, it is possible to explore the same ideas that are used for classical systems introducing the quantum concepts of measurement and system state.

In this section are described some important aspects of the decision theory applied on a quantum system based on the works of Helstrom [35, 36, 37].

3.1.1 Binary decision

Let's suppose that a quantum system can be only in two states described by the density operators $\boldsymbol{\Xi}_0$ and $\boldsymbol{\Xi}_1$ respectively with probabilities ζ and $1-\zeta$. An example can be the system consisting by the light aquired by the receiver in a optical on-off keying (OOK) communication system where the bit 0 is associated to the absence of light (vacuum state $\boldsymbol{\Xi}_0 = |0\rangle\langle 0|$) and the bit 1 is associated to the presence of coherent light (coherent state $\boldsymbol{\Xi}_1 = \boldsymbol{\Xi}(\mu)$) as represented in the figure 3.1. Note that the quantum system just described could be characterized by the density operator $\boldsymbol{\Xi} = \zeta\,\boldsymbol{\Xi}_0 + (1-\zeta)\,\boldsymbol{\Xi}_1$ but it is not useful for the following discussion.

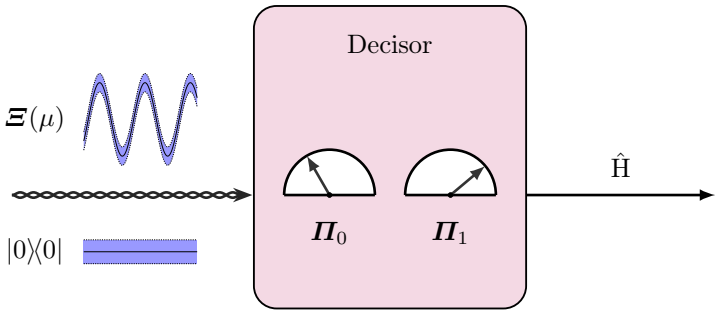

Figure 3.1: Schematic of a binary decision system involving a set of two POVM for the discrimination between a signal (coherent state $\boldsymbol{\Xi}(\mu)$) and the absence of signal (vacuum state $|0\rangle\langle 0|$).

The goal is to make a decision $\hat{\mathrm{H}}$ between two possible hypotheses: H_0 the density operator is $\boldsymbol{\Xi}_0$ and H_1 the density operator is $\boldsymbol{\Xi}_1$. The hypotheses are true with prior probabilies

$$f_{\mathsf{H}}(\mathrm{H}_0) = \mathbb{P}\{\mathrm{H}_0\} = \zeta; \tag{3.1a}$$

$$f_{\mathsf{H}}(\mathrm{H}_1) = \mathbb{P}\{\mathrm{H}_1\} = 1 - \zeta, \tag{3.1b}$$

and the choice of the hypothesis H_i when H_j is true (with $i, j \in \{0, 1\}$) has a cost C_{ij}. Suppose that a set of commuting observables $\{\boldsymbol{X}_i\}_{i=1,\dots,N}$ are measured in order to infer the right hypothesis and denote as $\{\mathsf{X}_i\}_{i=1,\dots,N}$ the outcomes of the measurement (note that they are random variables (RVs) due to two factors: the randomness of quantum measurements and the unknowness of the system). Classically, the decision is based on the value of a statistic of the outcomes, i.e., a function $f(x_1, x_2, \dots, x_N) : \mathbb{C}^N \to \mathbb{R}$ where $\mathbb{C}$ and $\mathbb{R}$ are respectively complex and real sets. Considering the quantum observables $\{\boldsymbol{X_i}\}_i$ of the system, it is possible to define the operator $\boldsymbol{\Pi} \coloneqq f(\boldsymbol{X}_1, \boldsymbol{X}_2, \dots, \boldsymbol{X}_N)$ with eigenvalues 1 and 0. The operator $\boldsymbol{\Pi}$ is called **detection operator**, is an observable of the system and its outcome correspond to the choice of one hypothesis. The optimal decision problem can be formulated as the problem to find the operator $\boldsymbol{\Pi}$ which ensure the best performance where performance can be quantified in several ways.

The firsts two common performance quantifiers are the false alarm probability and the missed-detection probability that are defined from the respective errors as it follows:

False alarm error occurs if the hypothesis H_1 is choosen when the right hypothesis is the H_0. The probability α of false alarm is then:

$$\alpha = \mathbb{P}\{1|\mathrm{H}_0\} = \mathrm{tr}\{\boldsymbol{\Xi}_0\, \boldsymbol{\Pi}\}. \tag{3.2}$$

Missed-detection error occurs if the hypothesis H_0 is choosen when the right one is the H_1. the probability β of missed-detection is:

$$\beta = \mathbb{P}\{0|\mathrm{H}_1\} = 1 - \mathrm{tr}\{\boldsymbol{\Xi}_1\, \boldsymbol{\Pi}\}. \tag{3.3}$$

The probabilities just defined are very easy and they can be useful in specific applications where a false alarm or a missed-detection is more relevent with respect to the other one. In this thesis is not described how to find the optimal detection operator considering one of the two previous probabilities as decision cost. However, is described how to define the optimal detection operator $\hat{\boldsymbol{\Pi}}$ that minimize the Bayesian risk, i.e.,

$$\hat{\boldsymbol{\Pi}} = \arg\min_{\tilde{\boldsymbol{\Pi}}} \mathscr{R}(\tilde{\boldsymbol{\Pi}}), \tag{3.4}$$

where $\mathscr{R}(\cdot)$ is the Bayesian risk, defined as

$$\mathscr{R}(\tilde{\boldsymbol{\Pi}}) \coloneqq \mathbb{E}_{\boldsymbol{\Xi},\,\mathsf{H}}\left\{C\left(\tilde{\boldsymbol{\Pi}},\,\mathsf{H}\right)\right\} \tag{3.5a}$$

$$= \zeta\,\left[C_{00}\;(1-\alpha) + C_{10}\,\alpha\,\right] + (1-\zeta)\,\left[C_{01}\,\beta + C_{11}\;(1-\beta)\right] \tag{3.5b}$$

$$= \zeta\,C_{00} + (1-\zeta)\;C_{01} - (1-\zeta)\,(C_{01}-C_{11})\;\mathrm{tr}\Big\{\boldsymbol{\Xi}_1\,\tilde{\boldsymbol{\Pi}} - \eta\,\boldsymbol{\Xi}_0\,\tilde{\boldsymbol{\Pi}}\Big\}, \tag{3.5c}$$

H is the binary RV that describes the hypotheses and their prior probability, and

$$\eta \coloneqq \frac{\zeta\;(C_{10}-C_{00})}{(1-\zeta)\,(C_{01}-C_{11})}. \tag{3.6}$$

To minimize the equation 3.5, assuming $C_{01} > C_{11}$ requires to maximize

$$\mathrm{tr}\Big\{\boldsymbol{\Xi}_1\,\tilde{\boldsymbol{\Pi}} - \eta\,\boldsymbol{\Xi}_0\,\tilde{\boldsymbol{\Pi}}\Big\} = \mathrm{tr}\Big\{(\boldsymbol{\Xi}_1 - \eta\,\boldsymbol{\Xi}_0)\,\tilde{\boldsymbol{\Pi}}\Big\} \tag{3.7}$$

over all the possible decision operators $\tilde{\boldsymbol{\Pi}}$. Called the operator's $\boldsymbol{\Xi}_1 - \eta\,\boldsymbol{\Xi}_0$ eigenvalues $\{\lambda_k\}_k$, i.e.,

$$(\boldsymbol{\Xi}_1 - \eta\,\boldsymbol{\Xi}_0)\;|\lambda_k\rangle = \lambda_k\,|\lambda_k\rangle\,, \tag{3.8}$$

the expression 3.7 can be written as

$$\mathrm{tr}\Big\{(\boldsymbol{\Xi}_1 - \eta\,\boldsymbol{\Xi}_0)\,\tilde{\boldsymbol{\Pi}}\Big\} = \sum_k \lambda_k\,\langle\lambda_k|\,\tilde{\boldsymbol{\Pi}}\,|\lambda_k\rangle\,. \tag{3.9}$$

The maximum value of 3.9 is obtained if

$$\langle\lambda_k|\,\tilde{\boldsymbol{\Pi}}\,|\lambda_k\rangle = 1 \qquad \text{if} \quad \lambda_k \geq 0 \tag{3.10a}$$

$$\langle\lambda_k|\,\tilde{\boldsymbol{\Pi}}\,|\lambda_k\rangle = 0 \qquad \text{if} \quad \lambda_k < 0. \tag{3.10b}$$

The best decision operator in terms of Bayesian risk, is then given by:

$$\boldsymbol{\Pi} = \sum_{k:\lambda_k\geq 0} |\lambda_k\rangle\langle\lambda_k|\,. \tag{3.11}$$

The error probabilities, using such operator, are given by (using 3.11 in 3.2 and 3.3)

$$\alpha = \sum_{k:\lambda_k\geq 0} \langle\lambda_k|\,\boldsymbol{\Xi}_0\,|\lambda_k\rangle\,, \tag{3.12a}$$

$$\beta = 1 - \sum_{k:\lambda_k\geq 0} \langle\lambda_k|\,\boldsymbol{\Xi}_1\,|\lambda_k\rangle \tag{3.12b}$$

and the minimum avarage cost is

$$C_{\min} = \min_{\tilde{\boldsymbol{\Pi}}} \mathscr{R}(\tilde{\boldsymbol{\Pi}}) = \zeta\,C_{00} + (1-\zeta)\,C_{01} - (1-\zeta)\,(C_{01}-C_{11}) \sum_{k:\lambda_k\geq 0} \lambda_k. \tag{3.13}$$

Choosing $C_{00} = C_{11} = 0$ and $C_{01} = C_{10} = 1$, the quantity $C_{\min}$ becomes the error probability $P_{e,min}$:

$$P_{\mathrm{e,\,min}} = \zeta\;\mathrm{tr}\Big\{\hat{\boldsymbol{\Pi}}\,\boldsymbol{\Xi}_0\Big\} + (1-\zeta)\left(1 - \mathrm{tr}\Big\{\hat{\boldsymbol{\Pi}}\,\boldsymbol{\Xi}_1\Big\}\right) \tag{3.14a}$$

$$= (1-\zeta) - (1-\zeta)\;\mathrm{tr}\Big\{\hat{\boldsymbol{\Pi}}\,(\boldsymbol{\Xi}_1 - \eta\,\boldsymbol{\Xi}_0)\Big\} \tag{3.14b}$$

$$= (1-\zeta)\left[1 - \sum_{k:\lambda_k\geq 0} \lambda_k\right] \tag{3.14c}$$

$$= (1-\zeta)\left[1 - \sum_k |\lambda_k| + \lambda_k\right] \tag{3.14d}$$

$$= \frac{(1-\zeta)}{2}\left(1 - \|\boldsymbol{\Xi}_1 - \eta\,\boldsymbol{\Xi}_0\|_1\right), \tag{3.14e}$$

where $\|\boldsymbol{A}\|_1 \coloneqq \sqrt{\boldsymbol{A}^\dagger \boldsymbol{A}}$ is the trace norm of $\boldsymbol{A}$ and if $\boldsymbol{A}$ is Hermitian (as the operator $\boldsymbol{\Xi}_1 - \eta\boldsymbol{\Xi}_0$ is):

$$\|\boldsymbol{A}\|_1 = \sum_k |\alpha_k|,$$

where $\{\alpha_k\}_k$ are the eigenvalues of $\boldsymbol{A}$.

A more common form of the equation 3.14 can be obtained denoting the prior probabilities of the hypotheses H_0 and H_1 respectively as p_0 and p_1:

$$P_{\mathrm{e,min}} = \frac{1}{2}\left(1 - \|p_1\boldsymbol{\Xi}_1 - p_0\boldsymbol{\Xi}_0\|_1\right). \tag{3.15}$$

This lower bound of the error probability is called **Helstrom bound**.

Finally, let's denote the eigenvalues of the density operators $\boldsymbol{\Xi}_0$ and $\boldsymbol{\Xi}_1$ by λ_{0k} and λ_{1k}, enumerated in descending order. If density operators $\boldsymbol{\Xi}_0$ and $\boldsymbol{\Xi}_1$ commute, the eigenvalues of $\boldsymbol{\Xi}_1 - \eta\boldsymbol{\Xi}_0$ are $\lambda_{1k} - \eta\lambda_{0k}$, and these are positives when $\frac{\lambda_{1k}}{\lambda_{0k}} > \eta$. The best procedure is then to measure either $\boldsymbol{\Xi}_0$ and $\boldsymbol{\Xi}_1$. When the system is found in the k-th common eigenstate, choose H_1 if $\frac{\lambda_{1k}}{\lambda_{0k}} \geq \eta$, H_0 in the other case. This procedure represent the quantum equivalent of the *likelihood ratio test*

$$\Lambda(\boldsymbol{x}) \coloneqq \frac{\mathscr{L}_{\boldsymbol{x}}(\mathrm{H}_1)}{\mathscr{L}_{\boldsymbol{x}}(\mathrm{H}_0)} \underset{\mathrm{H}_1}{\overset{\mathrm{H}_0}{\lessgtr}} \eta. \tag{3.16}$$

POVM formulation of the decision problem

It is also possible to formulate the problem of the decision between two states in terms of POVM as it follows. Given two hypothesis H_0 and H_1 defined as in the equation 3.1, we can define a set of two POVM $\boldsymbol{\Pi}_0$ and $\boldsymbol{\Pi}_1$ such that $\boldsymbol{\Pi}_0 + \boldsymbol{\Pi}_1 = \boldsymbol{I}$ and such that the probability of the measurement outcome i is

$$\mathbb{P}\{i\} = \mathrm{tr}\{\boldsymbol{\Pi}_0\,\boldsymbol{\Xi}\}. \tag{3.17}$$

The error probability results:

$$\begin{aligned} P_{\mathrm{e}} &= p_0\ \mathrm{tr}\{\boldsymbol{\Pi}_1\,\boldsymbol{\Xi}_0\} + p_1\ \mathrm{tr}\{\boldsymbol{\Pi}_0\,\boldsymbol{\Xi}_1\} && \text{(3.18a)}\\ &= p_0\ \mathrm{tr}\{\boldsymbol{\Pi}_1\,\boldsymbol{\Xi}_0\} + p_1\ \mathrm{tr}\{\boldsymbol{\Xi}_1\} - p_1\ \mathrm{tr}\{\boldsymbol{\Pi}_1\,\boldsymbol{\Xi}_1\} && \text{(3.18b)}\\ &= p_1 - \mathrm{tr}\{\boldsymbol{\Pi}_1\,(p_1\,\boldsymbol{\Xi}_1 - p_0\,\boldsymbol{\Xi}_0)\}, && \text{(3.18c)} \end{aligned}$$

where p_0 and p_1 are the prior probabilities of the hypothesis H_0 and H_1. The optimization of the equation 3.18 with respect to all possible POVMs gives us the optimal set of decision operators and the minimum value of the error probability $P_{\mathrm{e,min}}$. Similarly to the previous procedure, writing the trace in the eigenbasis of $p_1\,\boldsymbol{\Xi}_1 - p_0\,\boldsymbol{\Xi}_0$, $\{|\lambda_k\rangle\}$, the $P_{\mathrm{e,\,min}}$ can be obtained maximizing this trace:

$$\mathrm{tr}\{\boldsymbol{\Pi}_1\,(p_1\,\boldsymbol{\Xi}_1 - p_0\,\boldsymbol{\Xi}_0)\} = \sum_k \lambda_k\,\langle\lambda_k|\,\boldsymbol{\Pi}_1\,|\lambda_k\rangle\,. \tag{3.19}$$

It results that $\hat{\boldsymbol{\Pi}}_1$ (optimal operator) is the projection operator of the positive eigenvalues of $p_1\,\boldsymbol{\Xi}_1 - p_0\,\boldsymbol{\Xi}_0$, i.e.,

$$\boldsymbol{\Pi}_1 = \sum_{k:\lambda_k \geq 0} |\lambda_k\rangle\langle\lambda_k| \tag{3.20}$$

and $\hat{\boldsymbol{\Pi}}_0 = \boldsymbol{I} - \hat{\boldsymbol{\Pi}}_1$. Using the just defined optimal operators $\hat{\boldsymbol{\Pi}}_0$ and $\hat{\boldsymbol{\Pi}}_1$, the error probability lower bound is given by:

$$P_{\mathrm{e,min}} = \frac{1}{2}\left(1 - \|p_1\,\boldsymbol{\Xi}_1 - p_0\,\boldsymbol{\Xi}_0\|_1\right), \tag{3.21}$$

that is the **Helstrom bound** in the POVM formalism.

3.1.2 Quantum Chernoff bound

The **QCB** approximates the Helstrom bound 3.15 when it is possible to make N experiments in order to choice one of two hypotheses about the state of the quantum system $\boldsymbol{\Xi} \in \mathcal{H}$. The problem can be formulated as it follows

$$\mathrm{H}_0 : \boldsymbol{\Xi} = {\boldsymbol{\Xi}_0}^{\otimes N} \tag{3.22a}$$

$$\mathrm{H}_1 : \boldsymbol{\Xi} = {\boldsymbol{\Xi}_1}^{\otimes N} \tag{3.22b}$$

and the POVMs are defined on the product space $\mathcal{H}^{\otimes N}$. The Helstrom bound for the error probability results

$$P^{(N)}_{\mathrm{e,\,min}} = \frac{1}{2}\left(1 - \|p_1\,{\boldsymbol{\Xi}_1}^{\otimes N} - p_0\,{\boldsymbol{\Xi}_0}^{\otimes N}\|_1\right) \tag{3.23}$$

and if $N \to \infty$, it is possible to prove [38] that the equation 3.23 converges to

$$P^{(N)}_{\mathrm{e,\,min}} \sim e^{-N\,\xi_{\mathrm{QCB}}}; \tag{3.24}$$

where ξ_{QCB} is called **QCB** and is given by:

$$\xi_{\mathrm{QCB}} \coloneqq \lim_{N\to\infty} -\frac{\log\left(P^{(N)}_{\mathrm{e,\,min}}\right)}{N} \tag{3.25a}$$

$$= -\log\left(\min_{0\le s\le 1} \mathrm{tr}\left\{{\boldsymbol{\Xi}_1}^{s}\,{\boldsymbol{\Xi}_0}^{1-s}\right\}\right). \tag{3.25b}$$

Equivalentely, the equation 3.24 can be written as it follows:

$$P^{(N)}_{\mathrm{e,\,min}} \sim Q^N; \tag{3.26}$$

where

$$Q = \min_{0\le s\le 1} \mathrm{tr}\left\{{\boldsymbol{\Xi}_1}^{s}\,{\boldsymbol{\Xi}_0}^{1-s}\right\}. \tag{3.27}$$

Figure 3.2 compares the QCB and the Helstrom bound for the same hypothesis testing problem (the considered problem is the quantum illumination that will be described in the following chapter). It is possible to observe that the QCB is always greater then the Helstrom bound and it can be proven that converges to the last only for high values of N. The main advantage of the QCB is given by the less computational complexity with respect to the Helstrom bound due to the high dimensionality of ${\boldsymbol{\Xi}_i}^{\otimes N}$. For this reason, it is impossible to compute the Helstrom bound for higher values of N.

3.1.3 M-ary decision

The choice among M hypotheses of which the k-th asserts "The system is described by the density operator $\boldsymbol{\Xi}_k$", can be based on the outcome of a measurement described by M POVM $\{\boldsymbol{\Pi}_m\}_{m=1,\,\ldots,\,M}$ such that

$$\sum_{m=1}^{M} \boldsymbol{\Pi}_m = \boldsymbol{I}.$$

The problem is to find the set of operators $\{\boldsymbol{\Pi}_m\}_m$ that minimizes the avarage cost in the choice. Let ζ_k be the prior probability of the hypothesis H_k and let C_{ij} the cost of the choice H_i when H_j is true. As in the binary case, the Bayesian risk is given by:

$$\mathscr{R} = \sum_{i=1}^{M}\sum_{j=1}^{M} \zeta_i\,C_{ij}\ \mathrm{tr}\{\boldsymbol{\Xi}_j\,\boldsymbol{\Pi}_i\}. \tag{3.28}$$

The problem of minimizing 3.28 remains unsolved for $M > 2$. Only in particular cases a solution can be found (e.g., if hypotheses are related to pure states or if density operators commute) but their analysis is not topic of this thesis.

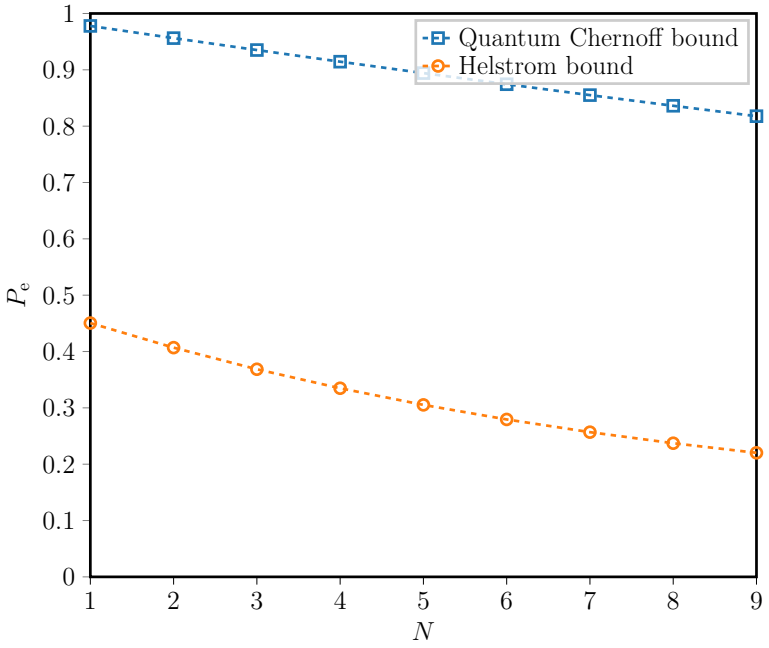

Figure 3.2: Comparison between the QCB and the Helstrom bound for a binary hypothesis test as a function of the number of experiments N.

3.2 Quantum Bayesian estimation theory

This section briefly describes the Bayesian estimation theory applied on quantum systems. Differently from the previously described decision theory, the estimation theory aims to infer the value of one or more unknown parameters which can take a continuous range of values. A typical use-case example is the estimation of the position of a target where a couple (in the 2D space) or a set of three coordinates (in the 3D space) are infered from distance informations.

In particular, quantum estimation theory aims to estimate a parameter $\boldsymbol{\vartheta}$ (that in general is a vector quantity) encoded in the state of a quantum system. The content of this section is based on the works of Helstrom [35, 37, 36].

3.2.1 Single parameter estimation

The simplest case of Bayesian estimation is to estimate a parameter $\theta \in \Theta$ where θ is a RV with prior distribution $f_\theta(\vartheta)$ and $\Theta \subset \mathbb{C}$. Let's suppose that parameter θ is encoded in the state of a quantum system $\boldsymbol{\Xi}(\theta)$. From the equation 2.2, follows that the state of the system can be written as:

$$\boldsymbol{\Xi} = \int_\Theta f_\theta(\vartheta)\, \boldsymbol{\Xi}(\vartheta) d\vartheta, \tag{3.29}$$

where $\boldsymbol{\Xi}(\vartheta)$ is the density operator of the state of the system if $\theta = \vartheta$. Let's estimate the parameter ϑ with $\hat{\vartheta}$ and then define an observable operator $\hat{\boldsymbol{\Theta}}$ such that the measurement outcome is $\hat{\vartheta}$. The estimation operator $\hat{\boldsymbol{\Theta}}$ is an infinite dimensional operator defined as:

$$\hat{\boldsymbol{\Theta}} = \int_\Theta \vartheta\, \boldsymbol{P}(\vartheta) d\vartheta, \tag{3.30}$$

where $\boldsymbol{P}(\vartheta)$ is the projection operator associated to the outcome ϑ and the operators $\boldsymbol{P}(\vartheta)$ have to satisfy the completness equation:

$$\int_\Theta \boldsymbol{P}(\vartheta)\, d\vartheta = \boldsymbol{I}\,. \tag{3.31}$$

Defining the optimal estimation operator $\hat{\boldsymbol{\Theta}}$ is then equivalent to define the optimal POVMs $\{\boldsymbol{P}(\vartheta)\}$ that minimize a decision cost. The decision cost is a function $\mathscr{C}\left(\tilde{\vartheta},\,\vartheta\right)$ that represents the cost of the choice of $\tilde{\vartheta}$ when the real value of the parameter is ϑ. The expected value of the estimation cost is then given by:

$$\mathbb{E}_{\tilde{\theta},\,\theta}\left\{\mathscr{C}\left(\tilde{\vartheta},\,\vartheta\right)\right\} = \iint_{\Theta^2} \mathscr{C}\left(\tilde{\vartheta},\,\vartheta\right)\, f_{\tilde{\theta},\,\theta}(\tilde{\vartheta},\,\vartheta)\, d\tilde{\vartheta}\, d\vartheta \tag{3.32a}$$

$$= \iint_{\Theta^2} \mathscr{C}\left(\tilde{\vartheta},\,\vartheta\right)\, f_{\theta}(\vartheta)\, f_{\tilde{\theta}|\theta}(\tilde{\vartheta}|\vartheta)\, d\tilde{\vartheta}\, d\vartheta \tag{3.32b}$$

and the conditional probability $f_{\tilde{\theta}|\theta}(\tilde{\vartheta}|\vartheta)$ is given by

$$f_{\tilde{\theta}|\theta}(\tilde{\vartheta}|\vartheta) = \mathrm{tr}\Big\{\boldsymbol{\Xi}(\vartheta)\,\boldsymbol{P}(\tilde{\vartheta})\Big\}\,. \tag{3.33}$$

Replacing 3.33 in 3.32 we obtain:

$$\mathbb{E}_{\tilde{\theta},\theta}\left\{\mathscr{C}\left(\tilde{\vartheta},\,\vartheta\right)\right\} = \iint_{\Theta^2} \mathscr{C}\left(\tilde{\vartheta},\,\vartheta\right)\, f_{\theta}(\vartheta)\ \mathrm{tr}\Big\{\boldsymbol{\Xi}(\vartheta)\,\boldsymbol{P}(\tilde{\vartheta})\Big\}\, d\tilde{\vartheta}\, d\vartheta\,. \tag{3.34}$$

The optimal $\{\boldsymbol{P}(\vartheta)\}$ are then operators that satisfy the equation 3.31 and such that:

$$\boldsymbol{P}(\vartheta) = \underset{\tilde{\boldsymbol{P}}(\vartheta)}{\arg\min}\ \mathbb{E}_{\tilde{\theta},\theta}\left\{\mathscr{C}\left(\tilde{\vartheta},\,\vartheta\right)\right\}. \tag{3.35}$$

As in classical estimation theory, it is useful to define estimator operators $\hat{\boldsymbol{\Theta}}$ with small or zero biases and, at the same time, incuring small mean square errors (MSEs). In quantum formalism, the bias of an estimation operator $\hat{\boldsymbol{\Theta}}$ (with outcome $\hat{\theta}$) of the parameter ϑ encoded in the density operator $\boldsymbol{\Xi}(\vartheta)$ is defined as

$$b(\vartheta) = \mathbb{E}\left\{\hat{\theta} - \vartheta\right\} = \mathrm{tr}\Big\{\hat{\boldsymbol{\Theta}}\,\boldsymbol{\Xi}(\vartheta)\Big\} - \vartheta = \langle\hat{\boldsymbol{\Theta}}\rangle - \vartheta. \tag{3.36}$$

and the MSE is

$$\mathbb{V}\left\{\hat{\theta}\right\} = \mathbb{E}\left\{\left(\hat{\theta} - \vartheta\right)^2\right\} \tag{3.37a}$$

$$= \mathbb{E}\left\{\hat{\theta}^2\right\} - 2\,\mathbb{E}\left\{\hat{\theta}\right\}\,\vartheta + \vartheta^2 \tag{3.37b}$$

$$= \mathrm{tr}\Big\{\hat{\boldsymbol{\Theta}}^2\,\boldsymbol{\Xi}(\vartheta)\Big\} - 2\,\vartheta\ \mathrm{tr}\Big\{\hat{\boldsymbol{\Theta}}\,\boldsymbol{\Xi}(\vartheta)\Big\} + \vartheta^2\ \mathrm{tr}\{\boldsymbol{\Xi}(\vartheta)\} \tag{3.37c}$$

$$= \mathrm{tr}\Big\{\left(\hat{\boldsymbol{\Theta}}^2 - 2\,\vartheta\,\hat{\boldsymbol{\Theta}} + \vartheta^2\,\boldsymbol{I}\right)\ \boldsymbol{\Xi}(\vartheta)\Big\} \tag{3.37d}$$

$$= \mathrm{tr}\Big\{\boldsymbol{\Xi}(\vartheta)\ \left(\hat{\boldsymbol{\Theta}} - \vartheta\,\boldsymbol{I}\right)^2\Big\} \tag{3.37e}$$

$$= \langle\left(\hat{\boldsymbol{\Theta}} - \vartheta\,\boldsymbol{I}\right)^2\rangle\,, \tag{3.37f}$$

where in the equation 3.37c was been used $\mathrm{tr}\{\boldsymbol{\Xi}(\Theta)\} = 1$ due to the fact that $\boldsymbol{\Xi}(\Theta)$ is a density operator. Moreover, in the equation 3.37e is used the following property of the trace operator: $\mathrm{tr}\{\boldsymbol{A}\,\boldsymbol{B}\} = \mathrm{tr}\{\boldsymbol{B}\,\boldsymbol{A}\}$. An operator that has zero bias and attains the minimum value of variance for all values of the parameter ϑ is said to have **uniformly minimum variance**.

3.2.2 The Cramér-Rao inequality

In classical estimation theory, a lower bound for variance of the estimator exists and is defined by the **Cramér-Rao lower bound** (or information inequality). Following lines briefly describe the classical CRB and then is introduced its quantum counterpart: the QCRB.

Let $\mathsf{T}(\mathbf{X})$ be an estimator of ϑ with limitated variance and $\mathbf{X}$ a set of measurements. The lower bound of variance of the estimator is:

$$\mathbb{V}\left\{\mathsf{T}(\mathbf{X})\right\} = \mathbb{E}_{\mathbf{X}}\left\{\left(\mathsf{T}(\mathbf{X}) - \vartheta\right)^2\right\} \geq \frac{\left[\psi'(\vartheta)\right]^2}{\mathscr{I}_{\mathbf{X}(\vartheta)}} = \frac{\left[1 + b'(\vartheta)\right]^2}{\mathscr{I}_{\mathbf{X}(\vartheta)}}, \tag{3.38}$$

where:

$$\psi(\vartheta) \coloneqq \mathbb{E}_{\mathbf{X}}\left\{\mathsf{T}(\mathbf{X})\right\} = \vartheta + b(\vartheta) \tag{3.39}$$

and the derivative $(\cdot)'$ is performed with respect to the parameter ϑ. The quantity $\mathscr{I}_{\mathbf{X}}(\vartheta)$ is called Fisher information of $\mathbf{X}$ for the parameter ϑ and is defined as it follows:

$$\mathscr{I}_{\mathbf{X}}(\vartheta) = \mathbb{E}_{\mathbf{X}}\left\{\left[\frac{\partial}{\partial\vartheta}\log f_{\mathbf{X}|\theta}(\boldsymbol{x}|\vartheta)\right]^2\right\}. \tag{3.40}$$

In the quantum estimation theory we can find an equivalent inequality as it follows.

Theorem 3.2.1 (QCRB)**.** *Let $\hat{\boldsymbol{\Theta}}$ be an estimation operator for the parameter ϑ and $\hat{\theta}$ the RV that models the measurement outcome. Let $\boldsymbol{\Xi}(\vartheta)$ be the density operator of the system. The QCRB is:*

$$\mathbb{E}\left\{\left(\hat{\theta} - \vartheta\right)^2\right\} = \mathrm{tr}\left\{\boldsymbol{\Xi}(\vartheta)\,\left(\hat{\boldsymbol{\Theta}} - \vartheta\,\boldsymbol{I}\right)^2\right\} \geq \frac{\left[1 + b'(\vartheta)\right]^2}{\mathrm{tr}\{\boldsymbol{\Xi}(\vartheta)\,\boldsymbol{L}^2\}} = \frac{\left[1 + b'(\vartheta)\right]^2}{\mathrm{tr}\left\{\frac{\partial}{\partial\vartheta}\left[\boldsymbol{\Xi}(\vartheta)\right]\,\boldsymbol{L}\right\}}, \tag{3.41}$$

*where $\boldsymbol{L}$ is the **symmetrized logarithmic derivative (SLD)** of $\boldsymbol{\Xi}(\vartheta)$ with respect to ϑ defined as the Hermitian operator such that:*

$$\{\boldsymbol{\Xi},\,\boldsymbol{L}\} = 2\,\frac{\partial\boldsymbol{\Xi}}{\partial\vartheta} \tag{3.42}$$

where $\{\cdot,\,\cdot\}$ is the anti-commutator.

The quantity

$$\mathscr{F}(\vartheta) \coloneqq \mathrm{tr}\big\{\boldsymbol{\Xi}(\vartheta)\,\boldsymbol{L}^2(\vartheta)\big\} = \big\langle\boldsymbol{L}^2(\vartheta)\big\rangle \tag{3.43}$$

is called **quantum Fisher information** and the QCRB can be written as:

$$\big\langle\left(\hat{\boldsymbol{\Theta}} - \vartheta\right)^2\big\rangle = \mathrm{tr}\left\{\boldsymbol{\Xi}\,(\vartheta)\,\left(\hat{\boldsymbol{\Theta}} - \vartheta\right)^2\right\} \geq \frac{\left[1 + b'(\vartheta)\right]^2}{\mathscr{F}(\vartheta)}. \tag{3.44}$$

An interesting observation is that it is also possible to evaluate the classical Fisher information in a quantum parameter estimation process and results that

$$\mathscr{I}_{\mathbf{X}}(\vartheta) \leq \mathscr{F}(\vartheta) \tag{3.45}$$

The quantum Fisher information is then an upper bound for the Fisher information as it embodies the optimization of the Fisher information over all the measurement operators. The QCRB represents then a more strictly bound respect to the classical one.

Finally, let's describe how the previous results can be written if N copies of the same system are avaibles and the measurement can be replied over all systems. The state of the composite system is given by

$$\boldsymbol{\Xi}_{\boldsymbol{N}}(\vartheta) = \boldsymbol{\Xi}(\vartheta)^{\otimes N} \tag{3.46}$$

and the estimation is done due to an estimation operator $\hat{\boldsymbol{\Theta}}_{\boldsymbol{N}}$ acting on the product Hilbert space $\mathcal{H}^{\otimes N}$ and the quantum Fisher information of it for the parameter ϑ is given by:

$$\mathscr{F}_N(\vartheta) = \mathrm{tr}\Big\{\big[\boldsymbol{L}^2(\vartheta)\big]^{\otimes N}\;\boldsymbol{\Xi}(\vartheta)^{\otimes N}\Big\} = N\;\mathrm{tr}\big\{\boldsymbol{L}^2(\vartheta)\,\boldsymbol{\Xi}(\vartheta)\big\} = N\,\mathscr{F}(\vartheta). \tag{3.47}$$

The QCRB then can be written as

$$\big\langle(\boldsymbol{\Theta}_{\boldsymbol{N}} - \vartheta)^2\big\rangle \geq \frac{\left[1 + b'(\vartheta)\right]^2}{N\,\mathscr{F}(\vartheta)}. \tag{3.48}$$

3.2.3 Multiple parameter estimation

The last estimation case that is described in this thesis is the multi-parameter estimation. In this paragraph the problem is formulated and is presented the generalized version of the QCRB [36].

Let's consider the vector of unknown parameters $\boldsymbol{\vartheta} = [\vartheta_1, \ldots, \vartheta_m]$ of a quantum system described by the density operator $\boldsymbol{\Xi}(\boldsymbol{\vartheta})$. Let $\hat{\boldsymbol{\Theta}}_j$ be the operator whose outcome is the estimated parameter ϑ_j and suppose that it is unbiased, i.e.,

$$\langle \hat{\boldsymbol{\Theta}}_j \rangle = \mathrm{tr}\Big\{ \hat{\boldsymbol{\Theta}}_j \, \boldsymbol{\Xi}(\boldsymbol{\vartheta}) \Big\} = \vartheta_j \, . \tag{3.49}$$

Defining

$$\boldsymbol{\delta}\hat{\boldsymbol{\Theta}}_j = \hat{\boldsymbol{\Theta}}_j - \vartheta_j \, \boldsymbol{I} \tag{3.50}$$

the operator that measures the error in the estimation of ϑ_j and differentiating the equation 3.49 respect ϑ_k, results

$$\delta_{jk} = \mathrm{tr}\left\{ \frac{\partial \boldsymbol{\Xi}(\boldsymbol{\vartheta})}{\partial \vartheta_k} \, \hat{\boldsymbol{\Theta}}_j \right\} \tag{3.51}$$

where δ_{jk} is the Kronecker's delta function. Since the trace of a density operator is equal to 1, then

$$0 = \mathrm{tr}\left\{ \frac{\partial \boldsymbol{\Xi}(\boldsymbol{\vartheta})}{\partial \vartheta_k} \, \vartheta_j \right\}, \tag{3.52}$$

and subtracting 3.52 from 3.49, results:

$$\delta_{jk} = \mathrm{tr}\left\{ \frac{\partial \boldsymbol{\Xi}(\boldsymbol{\vartheta})}{\partial \vartheta_k} \left(\hat{\boldsymbol{\Theta}}_j - \vartheta_j \, \boldsymbol{I} \right) \right\} = \mathrm{tr}\left\{ \frac{\partial \boldsymbol{\Xi}(\boldsymbol{\vartheta})}{\partial \vartheta_k} \, \boldsymbol{\delta}\hat{\boldsymbol{\Theta}}_j \right\} \tag{3.53a}$$

$$= \frac{1}{2} \, \mathrm{tr}\Big\{ \left[\boldsymbol{\Xi}(\boldsymbol{\vartheta}) \, \boldsymbol{L}_k + \boldsymbol{L}_k \, \boldsymbol{\Xi}(\boldsymbol{\vartheta}) \right] \, \boldsymbol{\delta}\hat{\boldsymbol{\Theta}}_j \Big\}, \tag{3.53b}$$

where $\boldsymbol{L}_k$ is the SLD related to the estimation operator $\hat{\boldsymbol{\Theta}}_j$.

Let's consider the two following real vectors: $\boldsymbol{z}^T = [z_1, \, z_2, \, \ldots, \, z_m]$ and $\boldsymbol{y}^T = [y_1, y_2, \ldots, y_m]$; where $(\cdot)^T$ denote the transposition operation. Combining the m^2 equations 3.53, it can be written the following one:

$$\sum_{k=1,\ldots,m} \sum_{j=1,\ldots,m} z_k \, \delta_{jk} \, y_j = \sum_{j=1,\ldots,m} z_j \, y_j = \boldsymbol{z}^T \boldsymbol{y} \tag{3.54a}$$

$$= \frac{1}{2} \, \mathrm{tr}\left\{ \sum_{k=1,\ldots,m} \sum_{j=1,\ldots,m} z_k \, \left[\boldsymbol{\Xi}(\boldsymbol{\vartheta}) \, \boldsymbol{L}_k + \boldsymbol{L}_k \, \boldsymbol{\Xi}(\boldsymbol{\vartheta}) \right] \, \boldsymbol{\delta}\hat{\boldsymbol{\Theta}}_j \, y_j \right\} \tag{3.54b}$$

$$= \frac{1}{2} \, \mathrm{tr}\{ \boldsymbol{\Xi}(\boldsymbol{\vartheta}) \, \boldsymbol{Z} \, \boldsymbol{Y} + \boldsymbol{Y} \, \boldsymbol{Z} \, \boldsymbol{\Xi}(\boldsymbol{\vartheta}) \} \tag{3.54c}$$

$$= \frac{1}{2} \, \mathrm{Re}\{ \mathrm{tr}\{ \boldsymbol{\Xi}(\boldsymbol{\vartheta}) \, \boldsymbol{Z} \, \boldsymbol{Y} \} \}, \tag{3.54d}$$

where

$$\boldsymbol{Z} = \sum_{k=1,\ldots,m} z_k \, \boldsymbol{L}_k,$$

$$\boldsymbol{Y} = \sum_{j=1,\ldots,m} y_j \, \boldsymbol{\delta}\hat{\boldsymbol{\Theta}}_j.$$

From the Cauchy-Schwarz inequality and $\mathrm{Re}\{\cdot\}^2 \leq |\cdot|^2$, applied in the equation 3.54, follows:

$$\left(\boldsymbol{z}^T \boldsymbol{z} \right)^2 = \left[\mathrm{Re}\{ \mathrm{tr}\{ \boldsymbol{\Xi}(\boldsymbol{\vartheta}) \, \boldsymbol{Z} \, \boldsymbol{Y} \} \} \right]^2 \leq \left| \mathrm{tr}\{ \boldsymbol{\Xi}(\boldsymbol{\vartheta}) \, \boldsymbol{Z} \, \boldsymbol{Y} \} \right|^2 \tag{3.56a}$$

$$= \left| \mathrm{tr}\Big\{ \boldsymbol{\Xi}(\boldsymbol{\vartheta})^{\frac{1}{2}} \, \boldsymbol{Z} \, \boldsymbol{Y} \, \boldsymbol{\Xi}(\boldsymbol{\vartheta})^{\frac{1}{2}} \Big\} \right|^2 \tag{3.56b}$$

$$\leq \mathrm{tr}\Big\{ \boldsymbol{\Xi}(\boldsymbol{\vartheta})^{\frac{1}{2}} \, \boldsymbol{Z} \, \boldsymbol{Z} \, \boldsymbol{\Xi}(\boldsymbol{\vartheta})^{\frac{1}{2}} \Big\} \, \mathrm{tr}\Big\{ \boldsymbol{\Xi}(\boldsymbol{\vartheta})^{\frac{1}{2}} \boldsymbol{\eta}\boldsymbol{\eta} \boldsymbol{\Xi}(\boldsymbol{\vartheta})^{\frac{1}{2}} \Big\} \tag{3.56c}$$

$$= \mathrm{tr}\big\{ \boldsymbol{\Xi}(\boldsymbol{\vartheta}) \, \boldsymbol{Z}^2 \big\} \, \mathrm{tr}\big\{ \boldsymbol{\Xi}(\boldsymbol{\vartheta}) \, \boldsymbol{Y}^2 \big\}, \tag{3.56d}$$

since the operators are Hermitian. Defining the matrices $\boldsymbol{A}$ and $\boldsymbol{B}$ with elements defined as it follows:

$$A_{ij} = \frac{1}{2}\,\mathrm{tr}\{\boldsymbol{\Xi}\,(\boldsymbol{L}_i\,\boldsymbol{L}_j + \boldsymbol{L}_j\,\boldsymbol{L}_i)\} = \mathrm{tr}\left\{\frac{\partial \boldsymbol{\Xi}}{\partial \vartheta_i}\,\boldsymbol{L}_j\right\} \tag{3.57a}$$

$$B_{ij} = \frac{1}{2}\,\mathrm{tr}\left\{\boldsymbol{\Xi}\,\left(\boldsymbol{\delta}\hat{\boldsymbol{\Theta}}_i\,\boldsymbol{\delta}\hat{\boldsymbol{\Theta}}_j + \boldsymbol{\delta}\hat{\boldsymbol{\Theta}}_j\,\boldsymbol{\delta}\hat{\boldsymbol{\Theta}}_i\right)\right\}, \tag{3.57b}$$

the inequality 3.56 can be rewritten as

$$\mathrm{tr}\left\{\boldsymbol{\Xi}(\boldsymbol{\vartheta})\,\boldsymbol{Y}^2\right\} = \boldsymbol{y}^T\,\boldsymbol{B}\,\boldsymbol{y} \geq \frac{\left(\boldsymbol{z}^T\,\boldsymbol{y}\right)^2}{\mathrm{tr}\{\boldsymbol{\Xi}(\boldsymbol{\vartheta})\,\boldsymbol{Z}^2\}} = \frac{\left(\boldsymbol{z}^T\,\boldsymbol{y}\right)^2}{\boldsymbol{z}^T\,\boldsymbol{A}\,\boldsymbol{z}}. \tag{3.58}$$

If the estimators $\hat{\boldsymbol{\Theta}}_j$ commute eachother, the matrix $\boldsymbol{B}$ is the covariance matrix of the estimators, i.e.,

$$B_{ij} = \langle \boldsymbol{\delta}\hat{\boldsymbol{\Theta}}_i\,\boldsymbol{\delta}\hat{\boldsymbol{\Theta}}_j \rangle\ .$$

In the other hand, if they do not commute, it is not possible to give an interpretation of the matrix $\boldsymbol{B}$. In particular, only its diagonal elements retain their validity as variance but it is necessary that measurements are made on separate systems with identical density operator (else, the Heisenberg inequality acts on the measurements). In commuting cases we can rewrite the equation 3.58 as

$$\boldsymbol{z}^T\,\boldsymbol{A}\,\boldsymbol{z} \geq \frac{\left(\boldsymbol{z}^T\,\boldsymbol{y}\right)^2}{\boldsymbol{y}^T\,\boldsymbol{B}\,\boldsymbol{y}} \tag{3.59}$$

and maximizing the right-hand side with respect to the components of $\boldsymbol{y}$ with the Cauchy-Schwarz inequality, we obtain

$$\frac{\left(\boldsymbol{z}^T\,\boldsymbol{y}\right)^2}{\boldsymbol{y}^T\,\boldsymbol{B}\,\boldsymbol{y}} = \frac{\left(\boldsymbol{z}^T\,\boldsymbol{B}^{-\frac{1}{2}}\,\boldsymbol{B}^{\frac{1}{2}}\,\boldsymbol{y}\right)^2}{\boldsymbol{y}^T\,\boldsymbol{B}\,\boldsymbol{y}} \leq \boldsymbol{z}^T\,\boldsymbol{B}^{-1}\,\boldsymbol{z}. \tag{3.60}$$

The equation 3.59 becomes:

$$\boldsymbol{z}^T\,\boldsymbol{B}^{-1}\,\boldsymbol{z} \leq \boldsymbol{z}^T\,\boldsymbol{A}\,\boldsymbol{z} \tag{3.61}$$

that is the **QCRB for multiple parameters estimation**. Finally, we can observe that the left-hand (imposed equal to a constant) represents the *concentration ellipsoid*.

Chapter 4

Quantum illumination protocol

QI is a protocol proposed in the 2008 by Seth Lloyd [7] that aims to detect the presence of a target in a noisy environment with lower error probability with respect to conventional target detection protocols. The main difficult to cope with is that the thermal noise has the same nature of the radiation used as signal to detect the target, i.e., is an electromagnetic radiation, and then the discrimination between noise and signal is a non-trivial task. Lloyd's work is based on the previous paper of Massimiliano Sacchi [39] about the optimal discrimination of quantum operators using entangled states.

This chapter will describe the QI protocol with single-photon radiations and will report the analysis of QI with general noise models investigated by Young et al. in [8]. The performance of the system was been numerically studied and the results will be described. Furthermore, it was been studied what happend if three or more entangled radiation are used to detect the target. Finally, the optimal tradeoff between the number of ancilla photons and the number of shoots will be discussed.

4.1 The QI detection system

The QI protocol provides an innovative approach to detect a target using couple of entangled radiations and it differs from CI protocols characterized by the use of single unentangled radiations. Figure 4.1 shows a schematic representation of QI systems' working principle and compares it with CI systems. Both systems use electromagnetic radiations to shoot the target (signal radiations) and try to estabilish the presence of it with electromagnetic receivers that detect the reflected radiations. Providing a description of the two systems in terms of QM formalism, the radiation is described by a density operator $\boldsymbol{\Xi}_{\mathrm{S}}$. Such radiations are represented in figures with a chain-line. Detection errors may occur due to two main factors:

- the presence of thermal noise; and
- the random nature of the target which does not reflect the radiation with an unitary probability.

Distinguish between signal radiation and thermal noise could be then a non-trivial task for the receiver and this is the reason why the QI protocol is formulated. The protocol proposes to introduce a second ancillary radiation (ancilla radiation) $\boldsymbol{\Xi}_{\mathrm{A}}$ directly transmitted to the receiver. The ancilla is initially entangled with the signal and the idea is that the correlation between the two radiations allow us to recognize the signal with a lower error probability.

From an experimental point-of-view, the two entangled radiations can be obtained with a laser beam incidents to a nonlinear crystal with internal Hamiltonian such that it acts like a

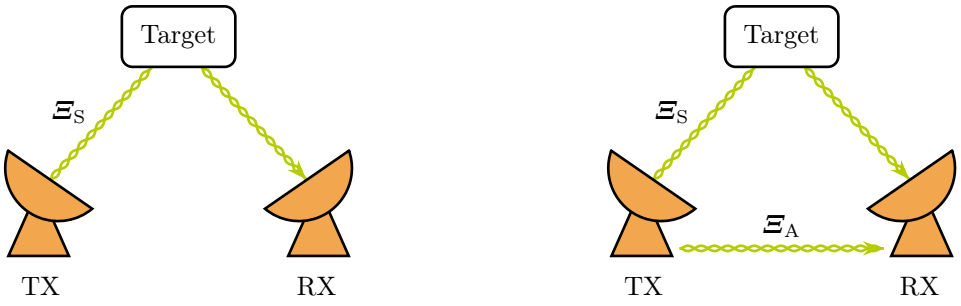

(a) CI detection system

(b) QI detection system

Figure 4.1: Schematic representations of the conventional and quantum illumination systems.

spontaneous parametric down-conversion (SPDC). An experimantal setup that implements the QI protocol was been tested in [10] using microwave radiations.

4.2 Quantum illumination with single-photon radiations

This section describes the QI protocol in the easiest case, i.e., when only one photon is sent to detect the target [7]. In this context, the considered radiations are represented simply by a Fock state $|1_k\rangle$ where the footer k means that the photon is in the k-mode, i.e., has energy $E = (1+\frac{1}{2})\,\hbar\,\omega_k$ (2.48). Considering the quantum system describing a d-modal electromagnetic radiation, a generic single-photon radiation quantum state can be written as it follows

$$|\mathrm{r}\rangle = \sum_{n_1=1}^{+\infty} \sum_{n_2=1}^{+\infty} \cdots \sum_{n_d=1}^{+\infty} r_{n_1 n_2 \ldots n_d}\, |n_1,\, n_2,\, \ldots,\, n_d\rangle \tag{4.1}$$

where $|n_1,\, n_2,\, \ldots,\, n_d\rangle = |n_1\rangle \otimes |n_2\rangle \otimes \cdots \otimes |n_d\rangle$ is the state of n_1 photons in the 1-mode, n_2 photons in the 2-mode, $\ldots$, n_d photons in the d-mode. The single-photon radiation with the photon in the k-mode is described by the state

$$|\psi\rangle = |0_1\rangle \otimes |0_2\rangle \otimes \cdots \otimes |1_k\rangle \otimes \cdots \otimes 0_d \tag{4.2}$$

nevertheless, in the following discussion about the QI, it will be denoted as $|k\rangle$ for simplicity.

In order to highlight the advantages of QI protocol, the next pages will compare two cases: CI where a single photon (signal photon) shoot the target and, if it is reflected, is received from a receiver antenna; QI where another photon (ancilla photon) in an entangled state with the signal one, is directly sent to the receiver and it is used to improve the performance int the detection of the signal photon. The reason why it is usefull to introduce the ancilla photon is that when the receiver obtain a photon it cannot know if it is the signal one or a thermal noise photon. The background idea is that the ancilla photon allows the receiver to discriminate between signal photon and noise photon with lower error probability thanks to the correlation (entanglement) with the first one.

The thermal noise that will be considered is described by the Planck's law 2.95 considering a multimodal radiation. In order to simplify the calculus, without loss of validity, a low-power noise is considered. The state of the thermal noise under the previous hypothesis can be written as:

$$\Xi_{\mathrm{th}} = (1 - d\,b)\; |0\rangle\langle 0| + b \sum_{k=1}^{d} |k\rangle\langle k| \tag{4.3}$$

where d is the number of considered modes (which is the number of modes that the receiver can detect. It depens on the listening time-window and on the bandwidth), b is the mean photon

number for each mode k (it is assumed to be constant), the state $|0\rangle$ is the vacuum state, i.e. the multimodal state $|0_1, 0_2, \ldots, 0_d\rangle$, and k is the single-photon state in the mode k described in the previous paragraph. Let analyze now the two cases presented before.

4.2.1 Single-photon CI

The problem to detect a target shooting it with a photon can be formulate in terms of hypothesis testing problem. In this case only one signal photon is considerend and no ancilla photons are used. This is the simplest quantum description of a conventional detector that use an electromagnetic radiation to shoot a target and perform a measurement to understand in the target has reflected the radiation. Let suppose that a single photon is sent and that the received photon is in a state $\boldsymbol{\Xi}_{\mathrm{r}} \in \{\boldsymbol{\Xi}_0, \boldsymbol{\Xi}_1\}$. Let define the two following hypotheses:

$$\mathrm{H}_0 : \text{The target is not there} \quad \Leftrightarrow \quad \boldsymbol{\Xi}_{\mathrm{r}} = \boldsymbol{\Xi}_0 \tag{4.4a}$$

$$\mathrm{H}_1 : \text{The target is there} \quad \Leftrightarrow \quad \boldsymbol{\Xi}_{\mathrm{r}} = \boldsymbol{\Xi}_1. \tag{4.4b}$$

and suppose that the prior probabilities of the two hypotheses are $p_0 = p_1 = 1/2$, i.e., the target is there with a probability $1/2$. Define the set of two optimal decision POVM $\boldsymbol{\Pi}_0$ and $\boldsymbol{\Pi}_1$ as described by Helstrom (3.20):

$$\boldsymbol{\Pi}_1 = \sum_{k:\lambda_k \geq 0} |\lambda_k\rangle\langle\lambda_k| \,, \tag{4.5a}$$

$$\boldsymbol{\Pi}_0 = \boldsymbol{I} - \boldsymbol{\Pi}_1; \tag{4.5b}$$

where $\{\, |\lambda_k\rangle \}_k$ are the eigenstate of $\boldsymbol{\Xi}_1 - \boldsymbol{\Xi}_0$ associated to the eigenvalues λ_k. The state $\boldsymbol{\Xi}_0$ is the state that we receive if the target is not there and then it is the state of the only thermal noise $\boldsymbol{\Xi}_{\mathrm{th}}$ as defined in 4.3, i.e.

$$\boldsymbol{\Xi}_0 = \boldsymbol{\Xi}_{\mathrm{th}} \,. \tag{4.6}$$

The target can be modelled in this context as a beam splitter with reflectivity factor η, i.e., a device that reflects a photon with a probability η and transmits it with a probability $1 - \eta$. If the target is there, the sent photon is in the state $\boldsymbol{\Xi} = |\psi\rangle\langle\psi|$, and a photon is received; then the density operator associated to the state of this photon is $\boldsymbol{\Xi}_1$ defined as:

$$\boldsymbol{\Xi}_1 = (1 - \eta)\, \boldsymbol{\Xi}_0 + \eta \boldsymbol{\Xi} \,. \tag{4.7}$$

The operator $\boldsymbol{\Xi}_1 - \boldsymbol{\Xi}_0$ results:

$$\boldsymbol{\Xi}_1 - \boldsymbol{\Xi}_0 = \eta\, (\boldsymbol{\Xi} - \boldsymbol{\Xi}_0) \tag{4.8a}$$

$$= \eta \left[|\psi\rangle\langle\psi| - (1 - d\, b)\, |0\rangle\langle 0| - b \sum_{k=1}^{d} |k\rangle\langle k| \right] \tag{4.8b}$$

$$= \eta \left[- (1 - d\, b)\, |0\rangle\langle 0| + (1 - b)\, |\psi\rangle\langle\psi| - b\, (\boldsymbol{I} - |\psi\rangle\langle\psi|) \right], \tag{4.8c}$$

where $\boldsymbol{I} = \sum_{k=1}^{d}$. The only positive eigenvalue of the operator just described is then $\lambda_i = 1 - b$ and then the decision operators result:

$$\boldsymbol{\Pi}_1 = |\psi\rangle\langle\psi| \tag{4.9a}$$

$$\boldsymbol{\Pi}_0 = \boldsymbol{I} - |\psi\rangle\langle\psi| \,. \tag{4.9b}$$

Studying all the probabilities correspondents to the facts of take the decision D_i when the hypothesis H_j is true (considering that the decision D_i is taken if the measurement related to

the just described POVM give the correspondent result), result:

$$\mathbb{P}\{\mathrm{D}_0|\mathrm{H}_0\} = \mathrm{tr}\{\boldsymbol{\Pi}_0\,\boldsymbol{\Xi}_0\} = 1-b; \tag{4.10a}$$
$$\mathbb{P}\{\mathrm{D}_1|\mathrm{H}_0\} = \mathrm{tr}\{\boldsymbol{\Pi}_1\,\boldsymbol{\Xi}_0\} = b; \tag{4.10b}$$
$$\mathbb{P}\{\mathrm{D}_0|\mathrm{H}_1\} = \mathrm{tr}\{\boldsymbol{\Pi}_0\,\boldsymbol{\Xi}_1\} = (1-b)(1-\eta); \tag{4.10c}$$
$$\mathbb{P}\{\mathrm{D}_1|\mathrm{H}_1\} = \mathrm{tr}\{\boldsymbol{\Pi}_1\,\boldsymbol{\Xi}_1\} = b\,(1-\eta)+\eta. \tag{4.10d}$$

The minimum decision error probability is given by the Helstrom bound 3.14 and results:

$$P_{\mathrm{e,\,min}} = \frac{1}{2}\left(1-\frac{1}{2}\left\|\boldsymbol{\Xi}_1-\boldsymbol{\Xi}_0\right\|_1\right) \tag{4.11a}$$
$$= \frac{1}{2}\left(1-\frac{1}{2}\,\eta\,(1-d\,b)-\frac{1}{2}\,\eta\,(1-b)-\frac{1}{2}\,\eta\,b\,(d-1)\right) \tag{4.11b}$$
$$= \frac{1}{2}\,(1-\eta+\eta\,b) \approx \frac{1}{2}\,(1-\eta)\,, \tag{4.11c}$$

where we have supposed that $\eta \ll 1$ and $b \ll 1$ ($\eta\,b \ll b, \eta$).

4.2.2 Single-photon QI

QI protocol proposes to use two entangled photons, one to shoot the target and one sent to the receiver as ancilla. In this paragraph is reported the protocol proposed by Lloyd describing how and when it can improve the detection performance.

Let $\boldsymbol{\Xi}_{\mathrm{r}} \in \{\boldsymbol{\Xi}_{\mathrm{SA}\,0}, \boldsymbol{\Xi}_{\mathrm{SA}\,1}\}$ be the state of the system composed by the received signal photon and the ancilla one. Let's define the two hypotheses about the target presence as it follows:

$$\mathrm{H}_0 : \text{The target is not there} \quad \Leftrightarrow \quad \boldsymbol{\Xi}_{\mathrm{r}} = \boldsymbol{\Xi}_{\mathrm{SA}\,0} \tag{4.12a}$$
$$\mathrm{H}_1 : \text{The target is there} \quad \Leftrightarrow \quad \boldsymbol{\Xi}_{\mathrm{r}} = \boldsymbol{\Xi}_{\mathrm{SA}\,1}. \tag{4.12b}$$

The states $\boldsymbol{\Xi}_{\mathrm{SA}\,0}$ and $\boldsymbol{\Xi}_{\mathrm{SA}\,1}$ are respectively the state of the system when the received photon can be only a thermal noise photon (no target) and the state of the system when the received photon could be the signal photon with a probability η and a thermal one with a probability $1-\eta$ (target there). Supposing that the state of the two entangled photons implemented by the transmitter is

$$|\psi_{\mathrm{SA}}\rangle = \frac{1}{\sqrt{d}}\sum_{k=1}^{d}|k_{\mathrm{S}},\,k_{\mathrm{A}}\rangle\,, \tag{4.13}$$

where $|k\rangle$ is the state of the single photon in the k-mode, the states $\boldsymbol{\Xi}_{\mathrm{SA}\,0}$ and $\boldsymbol{\Xi}_{\mathrm{SA}\,1}$ are given by:

$$\boldsymbol{\Xi}_{\mathrm{SA}\,0} = \boldsymbol{\Xi}_{\mathrm{th}} \otimes \frac{\boldsymbol{I}_{\mathrm{A}}}{d} = \frac{1-d\,b}{d}\,|0_{\mathrm{S}}\rangle\langle 0_{\mathrm{S}}| \otimes \boldsymbol{I}_{\mathrm{A}} + \frac{b}{d}\,\boldsymbol{I}_{\mathrm{SA}}; \tag{4.14a}$$
$$\boldsymbol{\Xi}_{\mathrm{SA}\,1} = (1-\eta)\,\boldsymbol{\Xi}_{\mathrm{SA}\,0} + \eta\,|\psi_{\mathrm{SA}}\rangle\langle\psi_{\mathrm{SA}}|\,. \tag{4.14b}$$

It is then possible to define the optimal detection POVM $\{\boldsymbol{\Pi}_0, \boldsymbol{\Pi}_1\}$ as:

$$\boldsymbol{\Pi}_1 = \sum_{k:\lambda_k \geq 0}|\lambda_k\rangle\langle\lambda_k| = |\psi_{\mathrm{SA}}\rangle\langle\psi_{\mathrm{SA}}|\,, \tag{4.15a}$$
$$\boldsymbol{\Pi}_0 = \boldsymbol{I}_{\mathrm{SA}} - \boldsymbol{\Pi}_1; \tag{4.15b}$$

where $\{\,|\lambda_k\rangle\}_k$ are the eigenstates of $\boldsymbol{\Xi}_{\mathrm{SA}\,1} - \boldsymbol{\Xi}_{\mathrm{SA}\,0}$ and the only one with positive correspondent eigenvalue is $|\psi_{\mathrm{SA}}\rangle$. The conditional probabilities of taking the decision D_i given that the true

hypothesis is H_j are given by:

$$\begin{aligned}
\mathbb{P}\{\mathrm{D}_0|\mathrm{H}_0\} &= \mathrm{tr}\{\boldsymbol{\Pi}_0\,\boldsymbol{\Xi}_{\mathrm{S}\,0}\} = 1-\mathrm{tr}\{\boldsymbol{\Pi}_1\,\boldsymbol{\Xi}_{\mathrm{S}\,0}\} && (4.16a)\\
&= 1-\mathrm{tr}\left\{\left[\frac{1-d\,b}{d}\;|0_{\mathrm{S}}\rangle\langle 0_{\mathrm{S}}|\otimes\boldsymbol{I}_{\mathrm{A}}+\frac{b}{d}\,\boldsymbol{I}_{\mathrm{SA}}\right]\;|\psi_{\mathrm{SA}}\rangle\langle\psi_{\mathrm{SA}}|\right\}\\
&= 1-\frac{b}{d^2}\;\mathrm{tr}\left\{\left[\sum_{\substack{k=1,\,\ldots,\,d\\ j=1,\,\ldots,\,d}}|k_{\mathrm{S}},\,k_{\mathrm{A}}\rangle\langle j_{\mathrm{S}},\,j_{\mathrm{A}}|\right]\left[\sum_{\substack{m=1,\,\ldots,\,d\\ n=1,\,\ldots,\,d}}|m_{\mathrm{S}},\,n_{\mathrm{A}}\rangle\langle m_{\mathrm{S}},\,n_{\mathrm{A}}|\right]\right\}\\
&= 1-\frac{b}{d^2}\;\mathrm{tr}\left\{\sum_{\substack{k=1,\,\ldots,\,d\\ j=1,\,\ldots,\,d}}|k_{\mathrm{S}},\,k_{\mathrm{A}}\rangle\langle j_{\mathrm{S}},\,j_{\mathrm{A}}|\right\}\\
&= 1-\frac{b}{d^2}\,d = 1-\frac{b}{d};\\
\mathbb{P}\{\mathrm{D}_1|\mathrm{H}_0\} &= \mathrm{tr}\{\boldsymbol{\Pi}_1\,\boldsymbol{\Xi}_{\mathrm{S}\,0}\} = \frac{b}{d}; && (4.16b)\\
\mathbb{P}\{\mathrm{D}_0|\mathrm{H}_1\} &= \mathrm{tr}\{\boldsymbol{\Pi}_0\,\boldsymbol{\Xi}_{\mathrm{S}\,1}\} = \left(1-\frac{b}{d}\right)(1-\eta); && (4.16c)\\
\mathbb{P}\{\mathrm{D}_1|\mathrm{H}_1\} &= \mathrm{tr}\{\boldsymbol{\Pi}_1\,\boldsymbol{\Xi}_{\mathrm{S}\,1}\} = \frac{b}{d}\,(1-\eta)+\eta. && (4.16d)
\end{aligned}$$

Note that all the error probability are decreased by a factor d with respect to the CI case (b is replaced by b/d everywhere). Finally, let's compute also the minimum error probability $P_{\mathrm{e,min}}$ with the Helstrom bound formula 3.14 as it follows. The operator $\boldsymbol{\Xi}_{\mathrm{SA}\,1}-\boldsymbol{\Xi}_{\mathrm{SA}\,0}$ results:

$$\begin{aligned}
\boldsymbol{\Xi}_{\mathrm{SA}\,1}-\boldsymbol{\Xi}_{\mathrm{SA}\,0} &= \eta\,\{\,|\psi_{\mathrm{SA}}\rangle\langle\psi_{\mathrm{SA}}|\;\boldsymbol{\Xi}_0\} && (4.17a)\\
&= \eta\left\{|\psi_{\mathrm{SA}}\rangle\langle\psi_{\mathrm{SA}}|-\frac{1-d\,b}{d}\;|0_{\mathrm{S}}\rangle\langle 0_{\mathrm{S}}|\otimes\boldsymbol{I}_{\mathrm{A}}-\frac{b}{d}\,\boldsymbol{I}_{\mathrm{SA}}\right\} && (4.17b)\\
&= \eta\left\{\left(1-\frac{b}{d}\right)\;|\psi_{\mathrm{SA}}\rangle\langle\psi_{\mathrm{SA}}|-\frac{1-d\,b}{d}\;|0_{\mathrm{S}}\rangle\langle 0_{\mathrm{S}}|\otimes\boldsymbol{I}_{\mathrm{A}}-\frac{b}{d}\;(\boldsymbol{I}_{\mathrm{SA}}-\;|\psi_{\mathrm{SA}}\rangle\langle\psi_{\mathrm{SA}}|)\right\}. && (4.17c)
\end{aligned}$$

Its eigenstates are $|\psi_{\mathrm{SA}}\rangle$, all the d eigenstates of $|0_{\mathrm{S}}\rangle\langle 0_{\mathrm{S}}|\otimes\boldsymbol{I}_{\mathrm{A}}$, i.e $\{\,|0_{\mathrm{S}},\,k_{\mathrm{A}}\rangle\}_k$, and all the d^2-1 eigenstates of $\boldsymbol{I}_{\mathrm{SA}}-\,|\psi_{\mathrm{SA}}\rangle\langle\psi_{\mathrm{SA}}|$. Its trace norm is then given by:

$$\begin{aligned}
\|\boldsymbol{\Xi}_{\mathrm{SA}\,1}-\boldsymbol{\Xi}_{\mathrm{SA}\,0}\|_1 &= \eta\left(1-\frac{b}{d}\right)+\eta\left(\frac{1-d\,b}{d}\right)d+\eta\,\frac{b}{d}\,(d^2-1) && (4.18a)\\
&= 2\,\eta\left(1-\frac{b}{d}\right) && (4.18b)
\end{aligned}$$

and then the minimum error probability results:

$$P_{\mathrm{e,min}} = \frac{1}{2}\left(1-\eta+\frac{\eta\,b}{d}\right). \tag{4.19}$$

We can observe that despite there is a little improvement in the error probability, it is very small because $\eta\,b \ll \eta, b$.

4.2.3 Multi-shot single-photon illumination

A more realistic implementation of the detection protocols described before needs to perform N shoots in order to detect the target and it is possible to show that, in this case, QI provides a significant performance improvement.

Eachone of the N transmission-reception event can be considered as indipendent from the others and then we can compute the minimum detection error probability with the QCB (3.26). In this section it is computed the QCB both using the CI protocol and QI.

Studing the CI with N shot, the operators $\boldsymbol{\Xi}_0$ and $\boldsymbol{\Xi}_1$ are given in the equations 4.6 and 4.7 and the QCB can be obtained given the following results

$$\boldsymbol{\Xi}_0{}^{1-s} = (1-d\,b)^{1-s}\ |0\rangle\langle 0| + b^{1-s}\,\boldsymbol{I} \tag{4.20a}$$

$$\begin{aligned}\boldsymbol{\Xi}_1{}^{s} &= (1-\eta)^s\,(1-d\,b)^s\ |0\rangle\langle 0| + (1-\eta)\,b\ (\boldsymbol{I} - |\psi\rangle\langle\psi|) + (b+\eta)^s\ |\psi\rangle\langle\psi| &\text{(4.20b)}\\ &\approx (1-\eta-d\,b)^s\ |0\rangle\langle 0| + (1-\eta)\,b\ (\boldsymbol{I} - |\psi\rangle\langle\psi|) + (b+\eta)^s\ |\psi\rangle\langle\psi|\,, &\text{(4.20c)}\end{aligned}$$

where the approximation done is $\eta\,b\,d \ll \eta,\, b$. The QCB then results:

$$\begin{aligned}Q &= \min_{0\le s\le 1} \mathrm{tr}\big\{\big[\boldsymbol{\Xi}_0{}^{1-s}\,\boldsymbol{\Xi}_1{}^{s}\big]\big\} &\text{(4.21a)}\\ &= \min_{0\le s\le 1} \mathrm{tr}\big\{\big[(1-d\,b)^{1-s}\,(1-\eta-d\,b)^s\ |0\rangle\langle 0| + b\ (\boldsymbol{I} - |\psi\rangle\langle\psi|) + (b+\eta)^s\,b^{1-s}\ |\psi\rangle\langle\psi|\big]\big\} &\text{(4.21b)}\\ &= \min_{0\le s\le 1}\left\{(1-d\,b)\left(\frac{1-\eta-d\,b}{1-d\,b}\right)^s + b\,(d-1) + b\left(\frac{b+\eta}{b}\right)^s\right\} &\text{(4.21c)}\\ &\approx \min_{0\le s\le 1}\left\{(1-d\,b)\left(1-\frac{s\,\eta}{1-d\,b}\right) + b\,d + b\left[-1+\left(1+\frac{\eta}{b}\right)^s\right]\right\} &\text{(4.21d)}\\ &= \min_{0\le s\le 1}\left\{1-s\,\eta + b\left[-1+\left(1+\frac{\eta}{b}\right)^s\right]\right\}. &\text{(4.21e)}\end{aligned}$$

Noticing that the error probability depends of η/b, it is possible to distinguish two working regimes: a **good regime** when $\eta/b > 1$, i.e., when a received photon is more probably the signal one, and a **bad regime** when $\eta/b < 1$. In the good regime limit case, when $\eta/b \gg 1$, the value of Q is obtaind for $s = \frac{\ln(\eta/b)}{\ln(1+\eta/b)} - \frac{\ln[\ln(1+\eta/b)]}{\ln(1+\eta/b)} \to 1$ and is

$$Q = 1 - \eta. \tag{4.22}$$

The result confirms that ${P_{\mathrm{e,min}}}^{(N)} = {P_{\mathrm{e,min}}}^{N}$. In the bad regime limit case, when $\eta/b \gg 1$ (or $b/\eta \gg 1$), the value of Q is obtained with $s \approx 1/2$ and it results

$$Q = 1 - \frac{1}{8}\,\frac{\eta^2}{b}. \tag{4.23}$$

Finally, let's study the case of N shoots QI. Let the state of the two entangled photons be $|\psi_{\mathrm{SA}}\rangle$. Using them in order to detect the target as described in the previous sections, it is possible to compute the minimum error probability with the QCB. Summarizing the result:

$$\boldsymbol{\Xi}_{\mathrm{SA}\,0}{}^{1-s} = \left(\frac{1-d\,b}{d}\right)^{1-s} |0_{\mathrm{S}}\rangle\langle 0_{\mathrm{S}}| \otimes \boldsymbol{I}_{\mathrm{A}} + \frac{b^{1-s}}{d^{1-s}}\,\boldsymbol{I}_{\mathrm{SA}}, \tag{4.24a}$$

$$\begin{aligned}\boldsymbol{\Xi}_{\mathrm{SA}\,1}{}^{s} &= \frac{(1-\eta)^s\,(1-d\,b)^s}{d^s}\ |0_{\mathrm{S}}\rangle\langle 0_{\mathrm{S}}| \otimes \boldsymbol{I}_{\mathrm{A}} + \frac{b^s}{d^s}\,(\boldsymbol{I}_{\mathrm{SA}} - |\psi_{\mathrm{SA}}\rangle\langle\psi_{\mathrm{SA}}|) + \left(\eta+\frac{b}{d}\right)^s\ |\psi_{\mathrm{SA}}\rangle\langle\psi_{\mathrm{SA}}| &\text{(4.24b)}\\ &\approx \frac{(1-s\eta)(1-d\,b)^s}{d^s}\ |0_{\mathrm{S}}\rangle\langle 0_{\mathrm{S}}| \otimes \boldsymbol{I}_{\mathrm{A}} + \frac{b^s}{d^s}\,(\boldsymbol{I}_{\mathrm{SA}} - |\psi_{\mathrm{SA}}\rangle\langle\psi_{\mathrm{SA}}|) + \left(\eta+\frac{b}{d}\right)^s\ |\psi_{\mathrm{SA}}\rangle\langle\psi_{\mathrm{SA}}| &\text{(4.24c)}\end{aligned}$$

and the product $\boldsymbol{\Xi}_0{}^{1-s}\,\boldsymbol{\Xi}_1{}^{s}$ becomes:

$$\boldsymbol{\Xi}_0{}^{1-s}\,\boldsymbol{\Xi}_1{}^{s} = \frac{1-d\,b}{d}\ |0_{\mathrm{S}}\rangle\langle 0_{\mathrm{S}}| \otimes \boldsymbol{I}_{\mathrm{A}} + \frac{b}{d}\,(\boldsymbol{I}_{\mathrm{SA}} - |\psi_{\mathrm{SA}}\rangle\langle\psi_{\mathrm{SA}}|) + \left(\frac{b}{d}\right)^{1-s}\left(\eta+\frac{b}{d}\right)^s\ |\psi_{\mathrm{SA}}\rangle\langle\psi_{\mathrm{SA}}|\,. \tag{4.25}$$

The QCB results then:

$$\begin{aligned}Q &= \min_{0\le s\le 1} \mathrm{tr}\big\{\big[\boldsymbol{\Xi}_0{}^{1-s}\,\boldsymbol{\Xi}_1{}^{s}\big]\big\} &\text{(4.26a)}\\ &\approx \min_{0\le s\le 1}\left\{1-\eta\,s + \frac{b}{d}\left[-1+\left(1+\frac{d\,\eta}{b}\right)^s\right]\right\}. &\text{(4.26b)}\end{aligned}$$

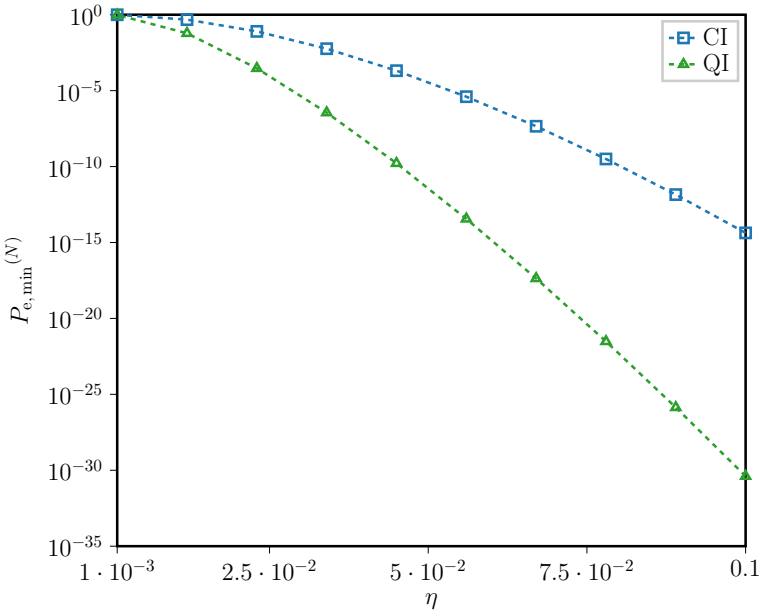

Figure 4.2: Comparison between CI and QI protocols as a function of η, fixed $b = 10^{-2}$, $d = 10$ and $N = 10^3$.

It is also possible to distinguish two new working regimes: a **good regime** with $d\,\eta/b > 1$ and a **bad regime** with $d\,\eta/b < 1$. In the limit case of the good regime $d\,\eta/b \gg 1$, the value of Q is obtained with $s \to 1$ and results the same QCB of the CI case:

$$Q = 1 - \eta\,. \tag{4.27}$$

However, in the limit case of the bad regime $d\,\eta/b \ll 1$, the QCB results

$$Q = 1 - \frac{\eta^2\,d}{8\,b} \tag{4.28}$$

and shows that the entanglement improves the performance of a d-factor in presence of high-noise, where d is the number of entangled modes. Measured in terms of e, i.e., the number of e-bits of entanglement, the enhancement of performance is $d = 2^e$.

In the figure 4.2 is plotted the detection error probability $P_{\mathrm{e,\,min}}{}^{(N)}$ in terms of the parameter η, fixed other variables b, N and d. QI has clearly a significant gain in terms of detection error probability performing multiple shoots.

4.3 Generic noise single-shot quantum illumination

A more general analysis of the single-shot quantum illumination was done in [8] where it is investigated the quantum illumination performance without the assumption of white noise and it is found the optimal joint state of ancilla and signal photons as a function of the noise characteristics. In this section are reported the most important results found.

The starting point of the analysis is to consider a single-photon noise (assumption of low-power) that is not white and that can be written as it follows

$$\boldsymbol{\Xi}_{\mathrm{E}} \approx b_0\ |0\rangle\langle 0| + \sum_{k=1}^{d} b_k\ |k\rangle\langle k|\,. \tag{4.29}$$

where the footer E means *environment state*, and describe it in its diagonal form

$$\boldsymbol{\Xi}_{\mathrm{E}} = \sum_{i=1}^{d} \vartheta_i\ |\vartheta_i\rangle\langle\vartheta_i|\,. \tag{4.30}$$

For convenince and without loss of generality, assume that $\vartheta_1 \geq \vartheta_2 \geq \cdots \geq \vartheta_d$. In the next paragraphs will be described the detection problem in case of CI and QI and there will be reported the best strategies that minimize the detection error probability.

4.3.1 Generic noise CI

In this section is described the detection of a target with a CI protocol and it is calculated the optimal state $\boldsymbol{\Xi}_{\mathrm{S}}$ that minimize the detection error probability $P_{\mathrm{e,\,min}}$. As in previous sections, the problem can be formulated in terms of binary hypothesis testing problem as it follows:

$$\mathrm{H}_0 : \ \boldsymbol{\Xi}_{\mathrm{r}} = \boldsymbol{\Xi}_{\mathrm{c},\,0} = \boldsymbol{\Xi}_{\mathrm{E}}, \tag{4.31a}$$

$$\mathrm{H}_1 : \ \boldsymbol{\Xi}_{\mathrm{r}} = \boldsymbol{\Xi}_{\mathrm{c},\,1} = (1-\eta)\,\boldsymbol{\Xi}_{\mathrm{E}} + \eta\,\boldsymbol{\Xi}_{\mathrm{S}}; \tag{4.31b}$$

where η is the beam splitter reflectivity factor, $\boldsymbol{\Xi}_{\mathrm{r}}$ is the received state and the footer c refers the CI. If the two hypotheses have respectively prior probabilities p_0 and p_1, the minimum detection error probability over all possible POVMs is given by the Helstrom Bound and results:

$$P_{\mathrm{e,\,min}} = \frac{1}{2}\left(1 - \|p_1\,\boldsymbol{\Xi}_{\mathrm{c},\,1} - p_0\,\boldsymbol{\Xi}_{\mathrm{c},\,0}\|_1\right) \tag{4.32a}$$

$$= \frac{1}{2}\left(1 - \|\boldsymbol{\Delta}_{\mathrm{c}}\|_1\right), \tag{4.32b}$$

where

$$\boldsymbol{\Delta}_{\mathrm{c}} \coloneqq p_1\,\boldsymbol{\Xi}_{\mathrm{c},\,1} - p_0\,\boldsymbol{\Xi}_{\mathrm{c},\,0} \tag{4.33a}$$

$$= p_1\,\eta\,\boldsymbol{\Xi}_{\mathrm{S}} + \left[p_1\,(1-\eta) - p_0\right]\,\boldsymbol{\Xi}_{\mathrm{E}} \tag{4.33b}$$

$$= p_1\,\eta\,\boldsymbol{\Xi}_{\mathrm{S}} + \gamma\,\boldsymbol{\Xi}_{\mathrm{E}}. \tag{4.33c}$$

The goal is minimize the $P_{\mathrm{e,\,min}}$ over all possible states $\boldsymbol{\Xi}_{\mathrm{S}}$ and then it is necessary to maximize $\|\boldsymbol{\Delta}_{\mathrm{c}}\|_1$ over all the possible photon states. Called **diamon norm** of $\boldsymbol{\Delta}_{\mathrm{c}}$ the following operator

$$\|\boldsymbol{\Delta}_{\mathrm{c}}\|_{\diamond} \coloneqq \max_{\boldsymbol{\Xi}_{\mathrm{S}}} \|\boldsymbol{\Delta}_{\mathrm{c}}\|_1 \tag{4.34}$$

and

$$P_{\mathrm{e},\,\diamond} \coloneqq \min_{\boldsymbol{\Xi}_{\mathrm{S}}} P_{\mathrm{e,\,min}} = \frac{1}{2}\left(1 - \|\boldsymbol{\Delta}_{\mathrm{c}}\|_{\diamond}\right). \tag{4.35}$$

it can be proven that the optimal states are always pure states ([8]), i.e $\boldsymbol{\Xi}_{\mathrm{S}} = |\psi_{\mathrm{S}}\rangle\langle\psi_{\mathrm{S}}|$. Furthermore, it is possible to distinguish three regions which achieve different error probabilities.

Region I: The region I is defined as the region with

1. $p_0 < p_1$,
2. $\eta < \eta_* \coloneqq 1 - p_0/p_1$, (equivalently $\gamma > 0$).

The error probability results $P_{\mathrm{e},\,\diamond} = p_0$ and can achieved with any state $\boldsymbol{\Xi}_{\mathrm{S}}$, pure or mixed. The decision strategy in this case is to say always that the hypothesis H_1 is true.

Region II: The region II is the dual of the first one and is defined as the region with

1. $p_0 > p_1$,
2. $\eta < \eta_c \coloneqq \left(\frac{p_0}{p_1} - 1\right)\left(\frac{\vartheta_d}{1-\vartheta_d}\right)$.

The minimum error probability results $P_{\mathrm{e},\,\diamond} = p_1$ and, similarly to the previous case, it can achieved with any state $\boldsymbol{\Xi}_{\mathrm{S}}$. The optimal strategy is to say that the true hypothesis is always the H_0.

Region III: The region III is the region excluded by the I and the II. The minimum error probability is $P_{\mathrm{e},\,\diamond} = p_0 + \gamma\,(1-\vartheta_d)$ and it is achieved choosing $|\psi_{\mathrm{S}}\rangle = |\vartheta_d\rangle$.

4.3.2 Generic noise QI

This section aims to describe how to find the optimal state $\boldsymbol{\Xi}_{\mathrm{SA}}$ of the composite system of the signal photon (S) and the ancilla one (A) that minimize the detection error probability $P_{\mathrm{e,\,min}}$. The two hypotheses can be formulated as it follows:

$$\mathrm{H}_0:\ \boldsymbol{\Xi}_{\mathrm{r}} = \boldsymbol{\Xi}_{\mathrm{q},\,0} = \boldsymbol{\Xi}_{\mathrm{E}} \otimes \boldsymbol{\Xi}_{\mathrm{A}}, \tag{4.36a}$$

$$\mathrm{H}_1:\ \boldsymbol{\Xi}_{\mathrm{r}} = \boldsymbol{\Xi}_{\mathrm{q},\,1} = (1-\eta)\,\boldsymbol{\Xi}_{\mathrm{E}} \otimes \boldsymbol{\Xi}_{\mathrm{A}} + \eta\,\boldsymbol{\Xi}_{\mathrm{SA}}; \tag{4.36b}$$

where q refers QI. If the two hypotheses have prior probabilities p_0 and p_1, the minimum error probability over all possible test POVMs is given by the Helstrom bound:

$$P_{\mathrm{e,\,min}} = \frac{1}{2}\left(1 - \|p_1\,\boldsymbol{\Xi}_{\mathrm{q},\,1} - p_0\,\boldsymbol{\Xi}_{\mathrm{q},\,0}\|_1\right) \tag{4.37a}$$

$$= \frac{1}{2}\left(1 - \|\boldsymbol{\Delta}_{\mathrm{q}}\|_1\right). \tag{4.37b}$$

Maximizing $P_{\mathrm{e,\,min}}$ over all possible states $\boldsymbol{\Xi}_{\mathrm{SA}}$, it is possible to find the optimal state of ancilla and signal photons. The result is discussed below defining three working regions as it follows.

Region I: The region I is defined, as in the conventional case, by

1. $p_0 < p_1$,
2. $\eta < \eta_* \coloneqq 1 - p_0/p_1$, (equivalently $\gamma > 0$).

The error probability and the decision strategies are the same as before, i.e., it results $P_{\mathrm{e},\,\diamond} = p_0$ and we can achieve this result with any state $\boldsymbol{\Xi}_{\mathrm{SA}}$, pure or mixed. The decision strategy is to say always that the hypothesis H_1 is true.

Region II: The region II is defined as the region with

1. $p_0 > p_1$,
2. $\eta < \eta_{\mathrm{c}} \coloneqq \left(\frac{p_0}{p_1} - 1\right)\left(\frac{\vartheta_h}{1-\vartheta_h}\right)$,

where

$$\vartheta_h{}^{-1} = \sum_i \vartheta_i{}^{-1}$$

and $\vartheta_h < \vartheta_d$. The minimum detection error probability results $P_{\mathrm{e},\,\diamond} = p_1$ and, similarly to the previous case, it can be achieved with any state $\boldsymbol{\Xi}_{\mathrm{SA}}$. The optimal strategy is to say that the true hypothesis is always the H_0.

Region III: The region III is the region excluded by I and II. The minimum detection error probability is $P_{\mathrm{e},\,\diamond} = p_0 + \gamma\,(1-\vartheta_h)$ and it is achieved choosing

$$|\psi_{SA}\rangle = \boldsymbol{I}_{\mathrm{S}} \otimes \boldsymbol{U}_{\mathrm{A}} \sum_{i=1}^{d} \mu_i\ |\vartheta_i,\,\vartheta_i\rangle\,, \tag{4.38}$$

where $\mu_i = \sqrt{\vartheta_h/\vartheta_i}$ and $\boldsymbol{U}_{\mathrm{A}}$ is a local unitary operator acting on the ancilla subsystem A. The optimal state's density operator is then given by $\boldsymbol{\Xi}_{\mathrm{SA}} = |\psi_{\mathrm{SA}}\rangle\langle\psi_{\mathrm{SA}}|$.

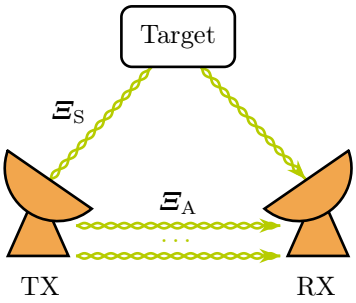

Figure 4.3: Schematic of the detection system using M entangled radiation.

4.4 Performance analysis of QI with M-photons per shoot

Finally, this section describes the major contribute of this thesis: the analysis of a QI-based protocol that use more then one ancillary single-photon radiations to detect the target. The analysis is performed in terms of QCB and the results will be shown in next lines. The goal is to identify, if exists, the optimal number of entangled photons M that minimize the detection error probability.

Figure 4.3 schematically describes the working principle of the system. The main idea is to use an M-modes entangled single-photons state in order to detect the target shooting it with one photon (signal photon) and sending the other $M-1$ (ancilla photons) to the receiver to perform a joint measurement on the multi-photon system.

In particular, let's suppose that the M photons are in the state

$$|\psi_{\mathrm{SA}}\rangle = \frac{1}{\sqrt{d}} \sum_{k=1}^{d} |k_{\mathrm{S}}, k_{\mathrm{A}_1}, \ldots, k_{\mathrm{A}_{M-1}}\rangle \,, \tag{4.39}$$

i.e., the state of M fully-entangled photons where $M-1$ are used as ancilla photons and one is used as signal to shoot the target (note that the state $|k\rangle$ represents the state of one single photon in k-mode, according to the previous sections definition). Let's suppose that N copies of the just defined state are avaiable. The hypotheses H_0 and H_1 associated respectively to the absence or the presence of the target can be formulated as it follows:

$$\mathrm{H}_0 : \ \boldsymbol{\Xi}_{\mathrm{r}} = \boldsymbol{\Xi}_{\mathrm{SA}\,0} = \boldsymbol{\Xi}_{\mathrm{th}} \otimes \mathrm{tr}_{\mathrm{s}} \{\boldsymbol{\Xi}_{\mathrm{SA}}\} \tag{4.40a}$$

$$\mathrm{H}_1 : \ \boldsymbol{\Xi}_{\mathrm{r}} = \boldsymbol{\Xi}_{\mathrm{SA}\,1} = (1-\eta)\, \boldsymbol{\Xi}_{\mathrm{SA}\,0} + \eta\, \boldsymbol{\Xi}_{\mathrm{SA}} \,, \tag{4.40b}$$

where $\boldsymbol{\Xi}_{\mathrm{th}}$ is the thermal state defined in the 4.3, $\mathrm{tr}_{\mathrm{s}}\{\cdot\}$ is the partial trace operator acting on the subsystem S that returns the reduced density operator of the ancillas subsystem, and $\boldsymbol{\Xi}_{\mathrm{SA}} = |\psi_{\mathrm{SA}}\rangle\langle\psi_{\mathrm{SA}}|$ is the state of the photons generated by the transmitter. The detection performance can be evaluated in terms of detection error probability with the QCB as it follows:

$$Q = \min_{0 \le s \le 1} \left\{ \boldsymbol{\Xi}_{\mathrm{SA}\,1}{}^{s}\, \boldsymbol{\Xi}_{\mathrm{SA}\,0}{}^{1-s} \right\} . \tag{4.41}$$

However, finding a closed form solution is not trivial due to the difficulty in diagonalizing the operator $\boldsymbol{\Xi}_{\mathrm{SA}\,1}{}^{s}\, \boldsymbol{\Xi}_{\mathrm{SA}\,0}{}^{1-s}$. In this thesis a simulative approach is used and figure 4.4 shows the results. The figure is obtained with the python tool QuTiP [40, 41] and plots the error probabilities (estimated with the QCB) as a function of M for different values of η. The value of d is setted to $d = 5$, b is fixed to $b = 10^{-2}$ and then the value of η fixes the ratio η/b. The budget of photons for the detection is $N_{\mathrm{B}} = 12000$ and the number of performed shoots is given by $N = N_{\mathrm{B}}/M$. The main difficult related to the performance estimation is given by the high-dimension of data that represent quantum states of composite systems. Indeed, the

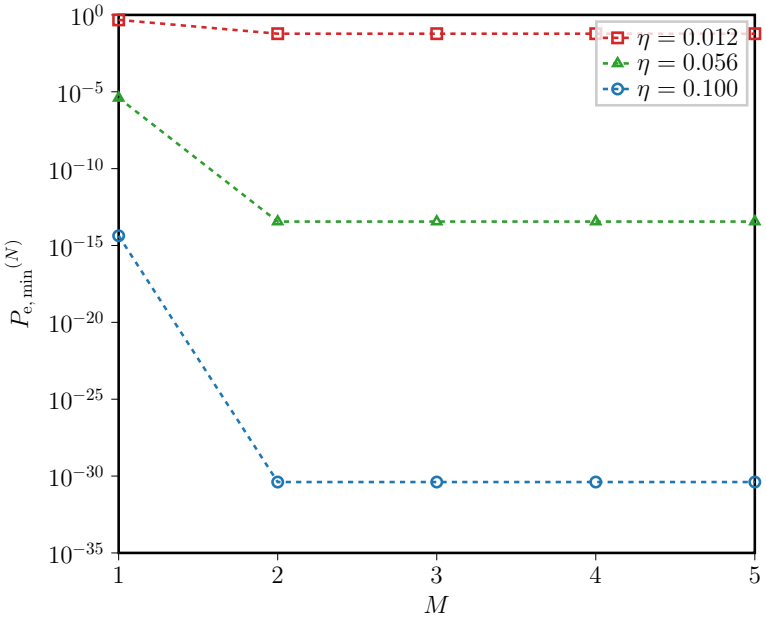

Figure 4.4: Error probability as a function of the number of radiations M for different values of η, fixed b and d and the photon budget N_{B}.

simulation of larger systems requires optimized algorithms and it is not possible to simulate systems characterized by high M.

In the figure it is clear that the optimal number of entangled photons for QI is two: one signal photon and one ancilla. The performace does not improve using two or more ancilla photons, even if the noise level is very high respect to the received signal (red line). Although the additional ancilla photons provide a little performance improvement, the reduction of the number of shoots fully offset it and the total error probability given the budget of photon does not decrease.

Finally, note that the previus conclusions consider an ideal transmitter with unitary generation efficience (given by the number of generated entangled photons over the total generated photons) and without generation noise. The study of a real system requires additional analysis and the results obtained in this thesis must be revised. Furthermore, the noise considered in the analysis is given by the equation 4.3 and further studies can be done considering more general noise models 4.29. Finally, similar analyses can be developed considering Gaussian and non-Gaussian quantum states instead of single-photon states.

Chapter 5

Conclusion

This thesis studied the QI protocol with single-photon states and generalized it to the case with mutiple ancilla photons. In particular, QI with single-photon states was presented as a hypothesis testing problem and the detection error probability was evaluated using decision theory. Then, QI was generalized for different noise models and multiple ancilla photons. Finally, the performance of QI with multiple ancilla photons was evaluated and the optimal tradeoff between the number of ancilla photons per shoot and the number of shoots was discussed.

Numerical results show that for a given budget of photons there exists an optimal number of ancilla photons that minimizes the detection error probability. The strategy that achieves the optimal performance is that one with one ancilla photon, even in the presence of noise.

The results obtained in this thesis represent a starting point to study non-ideal QI systems and additional quantum sensing protocols. Indeed, the methodologies used to describe and evaluate the QI protocol can alse be applied in the design of different quantum sensing applications including quantum tomography [14], quantum state discrimination (QSD) [3], and quantum communications [42].

Bibliography

[1] C. Degen, F. Reinhard, and P. Cappellaro, "Quantum sensing," *Rev. Mod. Phys.*, vol. 89, no. 3, Jul. 2017.

[2] A. Giani, M. Z. Win, and A. Conti, "Quantum discrimination of noisy photon-subtracted squeezed states," in *Proc. IEEE Global Commun. Conf.*, 2022, pp. 5826–5831.

[3] S. Guerrini, M. Z. Win, M. Chiani, and A. Conti, "Quantum discrimination of noisy photon-added coherent states," *IEEE J. Sel. Areas Inf. Theory*, vol. 1, no. 2, pp. 469–479, 2020.

[4] A. Giani, M. Z. Win, and A. Conti, "Quantum quadrature amplitude modulation with photon-added Gaussian states," in *Proc. IEEE Global Telecomm. Conf.*, Kuala Lumpur, Malaysia, 2023, to appear.

[5] S. Guerrini, M. Z. Win, and A. Conti, "Photon-varied quantum states: Unified characterization," *Phys. Rev. A*, vol. 108, no. 2, p. 022425, Aug. 2023.

[6] A. Giani, M. Z. Win, and A. Conti, "Source engineering for quantum key distribution with noisy photon-added squeezed states," in *Proc. IEEE Int. Conf. Commun.*, Rome, Italy, May 2023, to appear.

[7] S. Lloyd, "Enhanced sensitivity of photodetection via quantum illumination," *Science*, vol. 321, no. 5895, pp. 1463–1465, 2008.

[8] M.-H. Yung, F. Meng, X.-M. Zhang, and M.-J. Zhao, "One-shot detection limits of quantum illumination with discrete signals," *npj Quantum Inf.*, vol. 6, no. 1, p. 75, Sep. 2020.

[9] S. Pirandola and S. Lloyd, "Computable bounds for the discrimination of gaussian states," *Phys. Rev. A*, vol. 78, no. 1, Jul. 2008.

[10] S. Barzanjeh, S. Pirandola, D. Vitali, and J. M. Fink, "Microwave quantum illumination using a digital receiver," *Sci. Adv.*, vol. 6, no. 19, p. eabb0451, May. 2020.

[11] S. Tan, B. I. Erkmen, V. Giovannetti, S. Guha, S. Lloyd, L. Maccone, S. Pirandola, and J. H. Shapiro, "Quantum illumination with Gaussian states," *Phys. Rev. Lett.*, vol. 101, no. 25, Dec. 2008.

[12] Q. Zhuang, "Quantum ranging with gaussian entanglement," *Phys. Rev. Lett.*, vol. 126, no. 24, p. 240501, Jun. 2021.

[13] G. Tóth and I. Apellaniz, "Quantum metrology from a quantum information science perspective," *J. Phys. A*, vol. 47, no. 42, p. 424006, Oct. 2014.

[14] D. T. Smithey, M. Beck, M. G. Raymer, and A. Faridani, "Measurement of the Wigner distribution and the density matrix of a light mode using optical homodyne tomography: Application to squeezed states and the vacuum," *Phys. Rev. Lett.*, vol. 70, no. 9, pp. 1244–1247, Mar. 1993.

[15] J.-P. Chen, C. Zhang, Y. Liu, C. Jiang, D.-F. Zhao, W.-J. Zhang, F.-X. Chen, H. Li, L.-X. You, Z. Wang, Y. Chen, X.-B. Wang, Q. Zhang, and J.-W. Pan, "Quantum key distribution over 658 km fiber with distributed vibration sensing," *Phys. Rev. Lett.*, vol. 128, no. 18, p. 180502, May 2022.

[16] R. Jonsson and R. D. Candia, "Gaussian quantum estimation of the loss parameter in a thermal environment," *J. Phys. A*, vol. 55, no. 38, p. 385301, Aug. 2022.

[17] J. C. Chapman, J. M. Lukens, M. Alshowkan, N. Rao, B. T. Kirby, and N. A. Peters, "Coexistent quantum channel characterization using spectrally resolved Bayesian quantum process tomography," *Phys. Rev. Appl.*, vol. 19, no. 4, p. 044026, Apr. 2023.

[18] E. O. Ilo-Okeke, L. Tessler, J. P. Dowling, and T. Byrnes, "Entanglement-based quantum clock synchronization," *AIP Conf. Proc.*, vol. 2241, no. 1, p. 020011, Jun. 2020.

[19] Z. Wu, P. Wang, T. Wang, Y. Li, R. Liu, Y. Chen, X. Peng, R.-B. Liu, and J. Du, "Detection of arbitrary quantum correlations via synthesized quantum channels," *arXiv*, Jun. 2022.

[20] G. Chai, D. Li, Z. Cao, M. Zhang, P. Huang, and G. Zeng, "Blind channel estimation for continuous-variable quantum key distribution," *Quantum Eng.*, vol. 2, no. 2, p. e37, 2020.

[21] M. Planck, "Ueber irreversible strahlungsvorgänge," *Annalen der Physik*, vol. 306, no. 1, pp. 69–122, 1900.

[22] A. Einstein, "Über einen die erzeugung und verwandlung des lichtes betreffenden heuristischen gesichtspunkt," *Annalen der Physik*, vol. 322, no. 6, pp. 132–148, 1905.

[23] G. P. Thomson and A. Reid, "Diffraction of cathode rays by a thin film," *Nature*, vol. 119, no. 3007, pp. 890–890, Jun. 1927.

[24] A. Einstein, "Über die von der molekularkinetischen theorie der wärme geforderte bewegung von in ruhenden flüssigkeiten suspendierten teilchen," *Annalen der Physik*, vol. 322, no. 8, pp. 549–560, 1905.

[25] P. A. M. Dirac, *The Principles of Quantum Mechanics*. Oxford,: Clarendon Press, 1930.

[26] J. v. Neumann, *Mathematical foundations of quantum mechanics*. Princeton: Princeton University Press, 1932.

[27] M. A. Nielsen and I. L. Chuang, *Quantum Computation and Quantum Information*. Cambridge, U.K.: Cambridge University Press, 2010.

[28] A. Einstein, B. Podolsky, and N. Rosen, "Can quantum-mechanical description of physical reality be considered complete?" *Phys. Rev.*, vol. 47, pp. 777–780, May 1935.

[29] J. S. Bell, "On the Einstein Podolsky Rosen paradox," *Phys. Physique Fizika*, vol. 1, no. 3, pp. 195–200, Nov. 1964.

[30] J. F. Clauser, M. A. Horne, A. Shimony, and R. A. Holt, "Proposed experiment to test local hidden variable theories," *Phys. Rev. Lett.*, vol. 23, no. 15, pp. 880–884, Oct. 1969.

[31] A. Aspect, P. Grangier, and G. Roger, "Experimental realization of Einstein-Podolsky-Rosen-Bohm gedankenexperiment: A new violation of Bell's inequalities," *Phys. Rev. Lett.*, vol. 49, no. 2, pp. 91–94, Jul. 1982.

[32] I. Bialynicki-Birula, *Photon Wave Function*, ser. Progress in Optics, E. Wolf, Ed. Elsevier, 1996, vol. 36.

[33] J. Aasi et al., "Enhanced sensitivity of the LIGO gravitational wave detector by using squeezed states of light," *Nature Photon.*, vol. 7, no. 8, pp. 613–619, Aug. 2013.

[34] G. Cariolaro, *Quantum Communications*. Heidelberg, Germany: Springer, 2015.

[35] C. W. Helstrom, "Quantum detection and estimation theory," *J. Statist. Phys.*, vol. 1, no. 2, pp. 231–252, Jun. 1969.

[36] ——, "The minimum variance of estimates in quantum signal detection," *IEEE Trans. Inf. Theory*, vol. 14, no. 2, pp. 234–242, 1968.

[37] ——, "Minimum mean-squared error of estimates in quantum statistics," *Phys. Lett. A*, vol. 25, no. 2, pp. 101–102, 1967.

[38] K. M. R. Audenaert, J. Calsamiglia, R. Muñoz Tapia, E. Bagan, L. Masanes, A. Acin, and F. Verstraete, "Discriminating states: The quantum Chernoff bound," *Phys. Rev. Lett.*, vol. 98, no. 16, p. 160501, Apr. 2007.

[39] M. F. Sacchi, "Optimal discrimination of quantum operations," *Phys. Rev. A*, vol. 71, no. 6, Jun. 2005.

[40] J. Johansson, P. Nation, and F. Nori, "QuTiP 2: A Python framework for the dynamics of open quantum systems," *Comput. Phys. Commun.*, vol. 184, no. 4, pp. 1234–1240, 2013. [Online]. Available: https://www.sciencedirect.com/science/article/pii/S0010465512003955

[41] ——, "QuTiP: An open-source Python framework for the dynamics of open quantum systems," *Comput. Phys. Commun.*, vol. 183, no. 8, pp. 1760–1772, 2012. [Online]. Available: https://www.sciencedirect.com/science/article/pii/S0010465512000835

[42] S. Personick, "Application of quantum estimation theory to analog communication over quantum channels," *IEEE Trans. Inf. Theory*, vol. 17, no. 3, pp. 240–246, 1971.